




Astrophysics with New Horizons: Making the Most of a Generational Opportunity

Michael Zemcov^{1,2} , Iair Arcavi^{3,4}, Richard Arendt⁵, Etienne Bachelet⁴, Ranga Ram Chary⁶, Asantha Cooray⁷, Diana Dragomir⁸, Richard Conn Henry⁹, Carey Lisse¹⁰, Shuji Matsuura^{11,12}, Jayant Murthy¹³, Chi Nguyen¹, Andrew R. Poppe¹⁴, Rachel Street⁴, and Michael Werner²

¹ Center for Detectors, School of Physics and Astronomy, Rochester Institute of Technology, Rochester, NY 14623, USA; zemcov@cfdr.rit.edu

² Jet Propulsion Laboratory, 4800 Oak Grove Drive, Pasadena, CA 91109, USA

³ Einstein Fellow at the Department of Physics, University of California, Santa Barbara, CA 93106-9530, USA

⁴ Las Cumbres Observatory, 6740 Cortona Drive, Suite 102, Goleta, CA 93117-5575, USA

⁵ CRESST II/UMBC Observational Cosmology Laboratory, Code 665, Goddard Space Flight Center, 8800 Greenbelt Road, Greenbelt, MD 20771, USA

⁶ U.S. Planck Data Center, California Institute of Technology, 1200 East California Boulevard, Pasadena, CA 91125, USA

⁷ Department of Physics and Astronomy, University of California, Irvine, CA 92697, USA

⁸ NASA Hubble Fellow, Massachusetts Institute of Technology, Cambridge, MA 02139, USA

⁹ Henry A. Rowland Department of Physics and Astronomy, The Johns Hopkins University, Baltimore, MD 21218, USA

¹⁰ Planetary Exploration Group, Space Department, Johns Hopkins University Applied Physics Laboratory, 11100 Johns Hopkins Road, Laurel, MD 20723, USA

¹¹ School of Science and Technology, Kwansai Gakuin University, Sanda, Hyogo 669-1337, Japan

¹² Department of Space Astronomy and Astrophysics, the Institute of Space and Astronautical Science, Japan Aerospace Exploration Agency, Sagamihara, Kanagawa 252-5210, Japan

¹³ Indian Institute of Astrophysics, Bengaluru 560 034, India

¹⁴ Space Sciences Laboratory, University of California at Berkeley, Berkeley, CA, 94720, USA

Received 2018 February 23; accepted 2018 August 17; published 2018 September 28

Abstract

The outer solar system provides a unique, quiet vantage point from which to observe the universe around us, where measurements could enable several niche astrophysical science cases that are too difficult to perform near Earth. NASA's *New Horizons* mission comprises an instrument package that provides imaging capability from ultraviolet (UV) to near-infrared (near-IR) wavelengths with moderate spectral resolution located beyond the orbit of Pluto. A carefully designed survey with *New Horizons* can optimize the use of expendable propellant and the limited data telemetry bandwidth to allow several measurements, including a detailed understanding of the cosmic extragalactic background light; studies of the local and extragalactic UV background; measurements of the properties of dust and ice in the outer solar system; confirmation and characterization of transiting exoplanets; determinations of the mass of dark objects using gravitational microlensing; and rapid follow-up of transient events. *New Horizons* is currently in an extended mission designed to be focused on Kuiper Belt science that will conclude in 2021. The astrophysics community has a unique, generational opportunity to use this mission for astronomical observation at heliocentric distances beyond 50 au in the next decade. In this paper, we discuss the potential science cases for such an extended mission, and provide an initial assessment of the most important operational requirements and observation strategies it would require. We conclude that *New Horizons* is capable of transformative science, and that it would make a valuable and unique asset for astrophysical science that is unlikely to be replicated in the near future.

Key words: cosmic background radiation – diffuse radiation – Kuiper Belt: general – planets and satellites: detection – space vehicles – ultraviolet: ISM

Online material: color figures

1. Introduction

Astronomical observations have been performed from a wide range of locations, including the surface of Earth, from atmospheric platforms, and in space from orbit, as well as further afield like Earth's Lagrange points and from Earth-trailing orbits around the Sun. Very occasionally, humans have sent instruments to the outer edge of the solar system that are capable of astronomical observation (Weinberg et al. 1974; Broadfoot

et al. 1977; Weaver et al. 2008). These instruments have been used to make astronomical measurements, including studies of the decrease in the light from interplanetary dust (IPD) with heliocentric distance (Hanner et al. 1974), Ly α emission from the interplanetary medium (Gladstone et al. 2013); the diffuse light from the Galaxy (Toller et al. 1987; Gordon et al. 1998); the brightness of the cosmic optical background (COB; Toller 1983; Matsuoka et al. 2011; Zemcov et al. 2017) and the cosmic UV

background (CUB; Holberg 1986; Murthy et al. 1991, 1999; Edelstein et al. 2000); and the UV emission from specific objects (Holberg & Barber 1985), including studies of their spectral features (Murthy et al. 1993, 2001).

Over the years, a number of missions to the outer solar system including instrumentation expressly designed to obtain astrophysical measurements have been considered (e.g., Mather & Beichman 1996; Bock et al. 2012; Matsuura et al. 2014; Stone et al. 2015, among others). However, these missions are costly and difficult endeavors, and require positive funding environments. A more modest strategy is to take advantage of missions during their cruise phases when they are activated for system checks and calibration campaigns. This strategy maximizes science return by taking advantage of existing assets at only a modest increase in mission risk and complexity.

NASA’s *New Horizons* mission (Stern et al. 2008; Weaver et al. 2008) recently performed the first detailed reconnaissance of the Pluto-Charon system. *New Horizons* is currently in an extended mission designed to conduct a close fly-by investigation of the Kuiper Belt Object (KBO) 2014 MU69; perform unique observations of approximately two to three dozen other KBOs and Centaurs; and measure the heliospheric plasma, dust, and neutral gas environment out to a heliocentric distance of 50 au. This first extended mission phase is scheduled to conclude in the spring of 2021 (Stern et al. 2018). *New Horizons* includes as part of its instrument package the Long Range Reconnaissance Imager (LORRI; Cheng et al. 2008), the Multispectral Visible Imaging Camera (MVIC), the Linear Etalon Imaging Spectral Array (LEISA; Reuter et al. 2008) and an ultraviolet (UV) spectrograph Alice (Stern et al. 2008). In addition to their planetary imaging functions, these NH instruments can double as sensitive astronomical instruments working from the UV well into near-infrared (near-IR) wavelengths (see Figure 1).

New Horizons has generated a rich archival data set for both planetary studies and astronomy that is currently being analyzed. However, the spacecraft itself has operational capability significantly beyond its current mission, and could operate well into the heliopause. A tantalizing possibility is to use the *New Horizons* instruments for an extended mission for astrophysics where purposely designed observations can be performed. This would help maximize the science return from the mission, and would take advantage of this unique resource. Such an opportunity will not arise again in the foreseeable future.

In this paper, we outline the astrophysical studies that could be performed with the *New Horizons* instrument suite, focusing on measurements that require the exceptionally low foreground emission from the outer solar system, or the 50–100 au separation from Earth to the spacecraft. These include measurements of the diffuse UV/optical/near-IR backgrounds away from the obscuring effects of the Sun’s immediate environment, and careful photometry science including

exoplanet transits and microlensing that require an exceptionally stable platform. These concepts could be used to inform future science and uses of the *New Horizons* mission. In Section 2 we review the primary science cases that benefit from access to the outer solar system. We assess the sensitivity and stability of the instruments using pre-flight estimates and in-flight data in Section 3. In Section 4 we outline the operational requirements of these types of measurements, and describe a hypothetical astrophysical survey. Finally, Section 5 gives some concluding remarks and an outlook for the future.

The analysis of data and plotting in this paper are performed using custom routines in PYTHON and MATLAB; we use functionality from the SCIPY (Jones et al. 2001), NUMPY (Oliphant 2006), IPYTHON (Perez & Granger 2007), and MATPLOTLIB (Hunter 2007) libraries. As a note to assist readers unaccustomed to working with astrophysical surface brightness, throughout this paper we employ a convention for diffuse surface brightness given by λ_λ (sometimes called “intensity”), in which the specific intensity I_λ (which carries units power per unit area per unit solid angle per unit wavelength, e.g., $\text{nW m}^{-2} \text{sr}^{-1} \mu\text{m}^{-1}$) is multiplied by each λ . This definition is consistent with that used elsewhere in the astronomical community, but differs from some other fields, and is used because it succinctly describes the power one would measure with a detector with a narrow bandpass at at given wavelength. The quantity λ_λ is equal and equivalent to νI_ν , although I_ν itself carries units of power per unit area per unit solid angle per unit frequency (see e.g., Rybicki & Lightman 1986 for more details and derivations). Similarly, we choose a convention where we reference images to flux per 2.6 pixel² beam rather than per pixel, which only affects how diffuse surface brightnesses are calculated from raw data.

2. Astrophysical Science from the Outer Solar System

2.1. Measurement of the Extragalactic Background Light

The formation of stars and galaxies in the universe is accompanied by the release of photons from both gravitational and nuclear mechanisms (Hauser & Dwek 2001; Cooray 2016). A cosmic background radiation in the UV, optical, and IR parts of the electromagnetic spectrum is therefore an expected relic of structure formation processes, and measurements of these backgrounds provide insights into those processes. Practically speaking, the extragalactic background light (EBL) at optical/near-IR wavelengths is thought to be dominated by photons released by nucleosynthesis in stars, and constraints of this stellar emission integrated over cosmic history and can yield crucial insights into a variety of astrophysical phenomena. Specifically, precise measurement of the EBL enables a cosmic consistency test wherein the integrated light from all galaxies, stars, active galactic nuclei (AGN), and other point sources is compared with the EBL intensity (Tyson 1995). Any excess

component suggests the presence of new, diffuse sources of emission. Potential discoveries with profound implications for astronomy include the signature of diffuse recombination from the epoch of reionization (e.g., Matsumoto et al. 2005), the presence of intra-halo light in the diffuse intragalactic medium (e.g., Zemcov et al. 2014), and diffuse photons associated with dark matter annihilation and their products (e.g., Gong et al. 2016).

In the past, direct measurements of the EBL have been complicated by the presence of bright local foregrounds, including the Zodiacal light (ZL), diffuse galactic light (DGL), and the integrated starlight (ISL) arising from extended telescope response and faint stars (Leinert et al. 1998). Despite a great deal of interest, direct photometric measurement of the EBL has proved to be challenging, largely because the atmosphere and ZL are factors of ~ 100 brighter than the signal of interest. Though some progress has been made in accounting for these foregrounds in the optical (Bernstein 2007; Mattila et al. 2012) and into the near-IR (Gorjian et al. 2000; Wright 2001; Cambr esy et al. 2001; Wright 2004; Matsumoto et al. 2005; Levenson et al. 2007; Tsumura et al. 2013; Sano et al. 2015; Matsuura et al. 2017), small errors in this accountancy propagate to large errors on the inferred COB. As a result of misestimation of the foregrounds, the systematic errors of current photometric measurements of the EBL exceed the integrated light from all galaxies outside of our own (known as the integrated galactic light (IGL)) by a factors of at least several (e.g., Mattila 2003, 2006). It is desirable to measure the EBL from vantage points where the ZL is not an appreciable component of the diffuse sky brightness, such as the outer solar system or above the ecliptic plane (Cooray et al. 2009).

The surface brightness of the IPD light is thought to drop with heliocentric distance roughly as r^{-3} to levels significantly below the EBL by the orbit of Saturn (see Section 2.3). As a result, an EBL measurement from the outer solar system observing out of the plane of the ecliptic should not suffer from strong IPD light contamination. Indeed, data from the early NASA probes *Pioneer* 10 and 11 have been used to measure both the decrease in the IPD light with heliocentric distance (Hanner et al. 1974), the diffuse light from the Galaxy (Toller et al. 1987; Gordon et al. 1998), and the brightness of the COB itself (Toller 1983; Matsuoka et al. 2011) in two bands spanning 390–500 nm and 600–720 nm over heliocentric distances ranging from 1 to 5.3 au (Weinberg et al. 1974). Due to the large field of view and poor angular resolution of the *Pioneer* photometers, these measurements have uncertainties dominated by errors associated with subtracting galactic components. However, an instrument with fine angular resolution can easily mask stars to the level that their emission is negligible, and over modest fields of view tracers of galactic dust can be used to measure a correlation with the DGL component that can then be regressed from image. This

suggests that a 10 cm-class telescope in the outer solar system, coupled with a current understanding of the galactic emission components, would be ideal for measuring the EBL.

The *New Horizons* mission includes an instrument suite that is well suited to measurement of the EBL. Figure 2 shows the sensitivities of these instruments as compared to current measurements of the optical and near-IR backgrounds. LORRI is a Newtonian telescope with a 20.8 cm diameter Ritchey-Chr etien telescope, an 0.3×0.3 instantaneous field of view, $1'' \times 1''$ pixels, sensitivity over a broad 440–870 nm half-sensitivity passband, and (crucially) real-time dark current monitoring. The achieved point source sensitivity of LORRI is $V = 17$ (5σ) in a 10 s exposure in 4×4 pixel on-chip “rebinning” mode, making it a sensitive astronomical instrument for which the starlight that challenged earlier *Pioneer* measurements can be masked out. LORRI has lately been used to measure the brightness of the EBL in the optical, yielding an upper limit that rules out some of the highest previous measurements (Zemcov et al. 2017). However, that measurement was made on a very limited data set that was not optimized for precise measurements of the EBL, and significant improvements are possible. In even a limited 4-hour total integration time with LORRI, uncertainties similar to those on the IGL are expected. In fact, the ultimate error from a LORRI measurement is likely limited by our knowledge of the DGL and ISL foregrounds, rather than the intrinsic sensitivity of the instrument.

Similarly, MVIC is a broadband imaging instrument, but provides significantly more spectral information than LORRI. Compared to LORRI, each band has a long, thin field of view. This is not necessarily problematic for an EBL measurement, but the smaller aperture and narrower bandpass of the MVIC channels cause a factor of ~ 10 per-pixel sensitivity penalty for measuring the average sky brightness compared with LORRI. However, averaging over the array will help, and MVIC observations remain a promising way to gain crucial spectral information on the shape of the EBL spectrum throughout the optical, which would provide compelling information compared with a single LORRI data point over a similar wavelength range.

LEISA would make simultaneously the most interesting and challenging measurement of the EBL. The near-IR 1–3 μm background has proved very difficult to measure from Earth, and is very interesting as the light from the earliest galaxies will be redshifted into this range. LEISA provides detailed spectral information that could be used to search for e.g., the spectral bump expected from Lyman emission from the galaxies that reionized the universe (Cooray et al. 2004). However, LEISA has a relatively small aperture and $R = 240$ spectral resolution, making the per-pixel sensitivity poor. Significant integration time would be required to make a constraining measurement of the EBL.

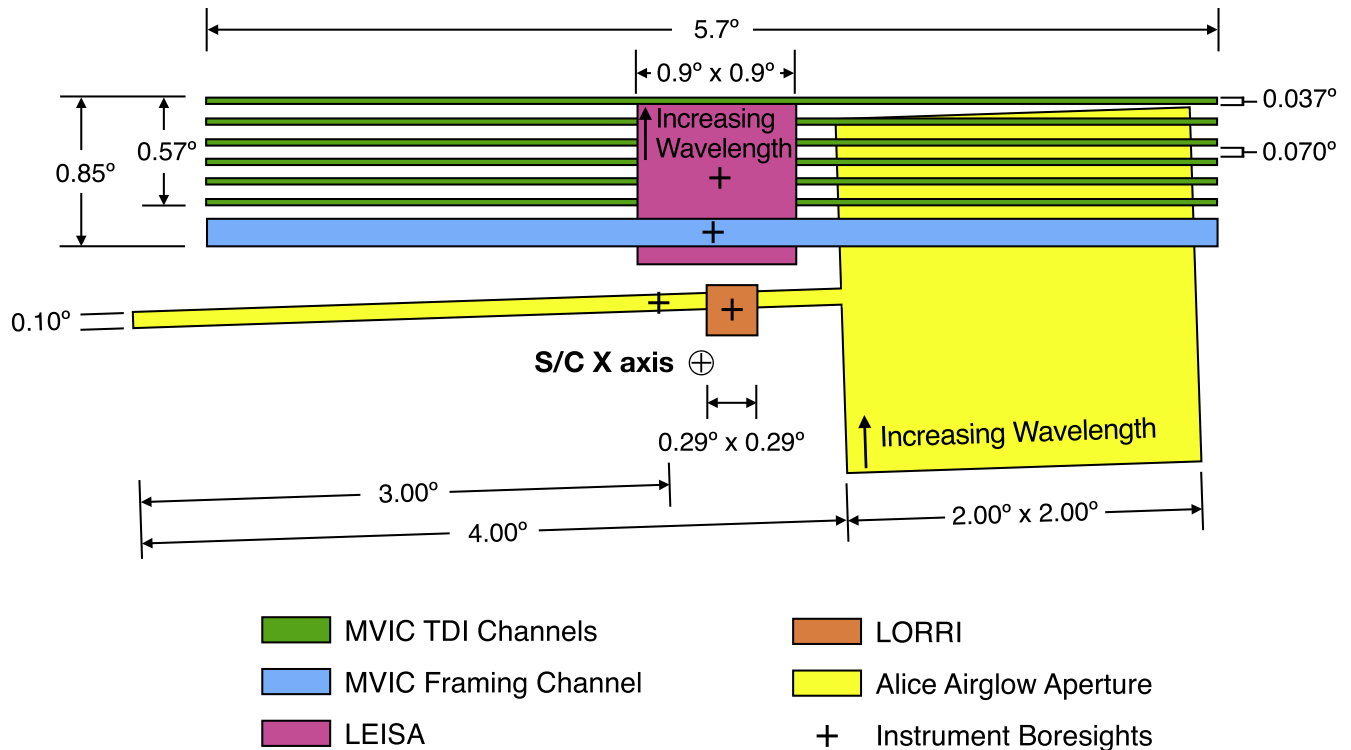


Figure 1. Layout of the focal plane of the imaging instruments on *New Horizons* (Weaver et al. 2008). LORRI has broad bandwidth, but has a relatively small footprint on the sky. MVIC observes in several colors in thin, long strips, while LEISA and Alice have relatively large fields of view. The instrument parameters are summarized in Table 1.

(A color version of this figure is available in the online journal.)

2.2. Measurement of the Ultraviolet Background

A detailed accounting of the cosmic ultraviolet background can provide information on a variety of astrophysical processes in the local interstellar medium (ISM) and other galaxies, including line emission and fluorescence from interstellar gas, high-energy light scattered by dust, the possibility of a massive hot halo of our own galaxy, and constraints on an extragalactic component interesting for reasons similar to those of the EBL discussed above. Despite the science impact, the interpretation of actual observations of the cosmic ultraviolet background has been controversial for more than a quarter of a century (see e.g., Bowyer 1991 and Henry 1991 for contrasting viewpoints). This is primarily because it is challenging to separate the different components of the diffuse emission, particularly with imaging surveys. Any spacecraft in low Earth orbit (e.g., *GALEX*) will be affected by airglow, while any spacecraft observing within the inner Solar System will be affected by the Lyman lines from interplanetary hydrogen and ZL at longer wavelengths. Even if we can account for these foregrounds, distant sources of astrophysical emission are difficult to separate without spectral diagnostics (Murthy 2009).

Almost all of our knowledge of the diffuse UV background in the spectral region longer than 1300 Å has come from *GALEX* broadband data. With only imaging data available, Murthy (2016) found that most of the diffuse radiation was due to scattered starlight, albeit with an offset of unknown origin (Hamden et al. 2013; Henry et al. 2015; Akshaya et al. 2018; Henry et al. 2018). However, the different components are impossible to separate photometrically, and the resulting backgrounds are highly model-dependent. In principle, spectroscopic observations from interplanetary space would allow a separation of the components. Murthy et al. (2001) used observations from the *Voyager* ultraviolet spectrographs (UVS) to observe that the diffuse background at shorter wavelengths ($\lambda < 1200$ Å) is patchy, and demonstrates a poor correlation with the diffuse background in the near-ultraviolet (NUV). The conclusion of this work is that although the two *Voyager* spacecraft observed far from the Sun, thereby avoiding airglow, they were still affected by the interplanetary HI lines. Instrumental scattering from interplanetary Ly α was the source of signal in many regions of the sky and affected the entire spectrum. This was compounded by the relatively low spectral resolution of 27 Å, so that the Ly α (1215 Å) and Ly β (1027 Å) lines were spread through much of the wavelength

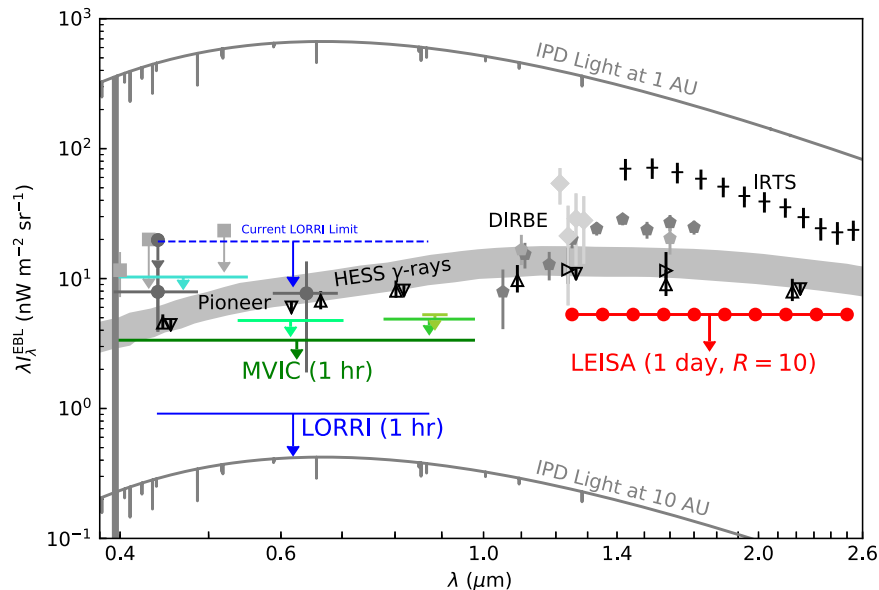


Figure 2. Measurements of the EBL surface brightness $\lambda\lambda^{\text{EBL}}$ in the optical and near-IR, including existing direct photometric constraints on the EBL (filled symbols) and the integrated galactic light (IGL; open symbols). We show the expected sensitivity of LORRI in $t_{\text{int}} = 1$ hour of integration time (blue limit), MVIC in $t_{\text{int}} = 1$ hour (green limits, one for each band), and LEISA in $t_{\text{int}} = 1$ day (red limits), as well as the existing 2σ upper limit from LORRI (blue dashed line; Zemcov et al. 2017). We show direct measurements of the EBL from observations using the “dark cloud” method (squares; Mattila et al. 2017), *Pioneer* 10/11 measurements (circles; Toller 1983; Matsuoka et al. 2011), CIBER (pentagons; Zemcov et al. 2014; Matsuura et al. 2017), combinations of DIRBE and 2MASS (diamonds; Wright 2001; Cambrésy et al. 2001; Wright 2004; Levenson et al. 2007), and IRTS (plus symbols; Matsumoto et al. 2005). The shaded region indicates the HESS γ -ray constraints on the extragalactic background light (H.E.S.S. Collaboration et al. 2013). The IGL points are compiled from the Hubble Deep Field (downward open triangles; Madau & Pozzetti 2000) and the Subaru Deep Field (upward open triangles and sideways pointing triangles; Totani et al. 2001; Keenan et al. 2010) in the optical/near-IR. The diffuse galactic light is a foreground associated with dust in the Milky Way galaxy that reaches a minimum of about $5 \text{ nW m}^{-2} \text{ sr}^{-1}$, but can be subtracted using various means. Ultimately, even modest integration times could permit definitive measurements of the brightness of the EBL over 3 octaves in frequency.

(A color version of this figure is available in the online journal.)

range between $900\text{--}1200 \text{ \AA}$. This problem is exacerbated in the extraction of the background line emission (Murthy et al. 1993, 2001).

The advantage of *New Horizons* is that observations will be made from outside the orbit of Pluto, more than 50 au away. Although instrumental scattering of interplanetary Ly α is still a problem, the magnitude of the line drops by an order of magnitude from 1 au to 50 au (Murthy et al. 2001). The 9 \AA resolution of Alice is well suited to search for diffuse emission from the Galaxy, both continuum and in lines. This is because both the foreground scattered from the interplanetary HI lines is minimized through observations from the outer solar system, and that the spectral shape of the astrophysical emission components can be used to decompose the emission. For example, emission from the Lyman and Werner bands of molecular hydrogen will extend throughout the UV in regions of high density, while diffuse OVI ($1032/1038 \text{ \AA}$) emission will track the hot gas (Dixon et al. 2006). These can be used to understand the local ISM through observations of different parts of the sky. Finally, the dust scattered starlight should correlate with the positions of the emitting O and B stars. Residuals should be due to extragalactic emission at high

latitudes or to a previously unknown emissive component at low galactic latitudes.

2.3. Edgeworth-Kuiper Belt Dust

Interplanetary dust particles are generated by several sources including comets, asteroids, and Edgeworth-Kuiper Belt (EKB) objects and range in size from $\sim 0.1 \mu\text{m}$ up to 1 mm. After ejection from their parent bodies, IPD particles diffuse through the solar system as they are affected by a variety of forces such as gravitation, Poynting-Robertson drag, solar radiation pressure, and solar wind drag (e.g., Burns et al. 1979; Gustafson 1994). As these grains encounter planetary systems, they have significant impacts on a wide range of planetary processes, such as the alteration of atmospheric photochemistry (e.g., Moses 1992; Feuchtgruber et al. 1997; Moses et al. 2000; Frankland et al. 2016; Moses & Poppe 2017); the injection of metallic species into planetary magnetospheres (Christon et al. 2015); the spatial and compositional evolution of Saturn’s main ring system (e.g., Durisen et al. 1989; Cuzzi & Estrada 1998; Estrada et al. 2015); and the production of impact ejecta clouds and/or rings from airless bodies, like

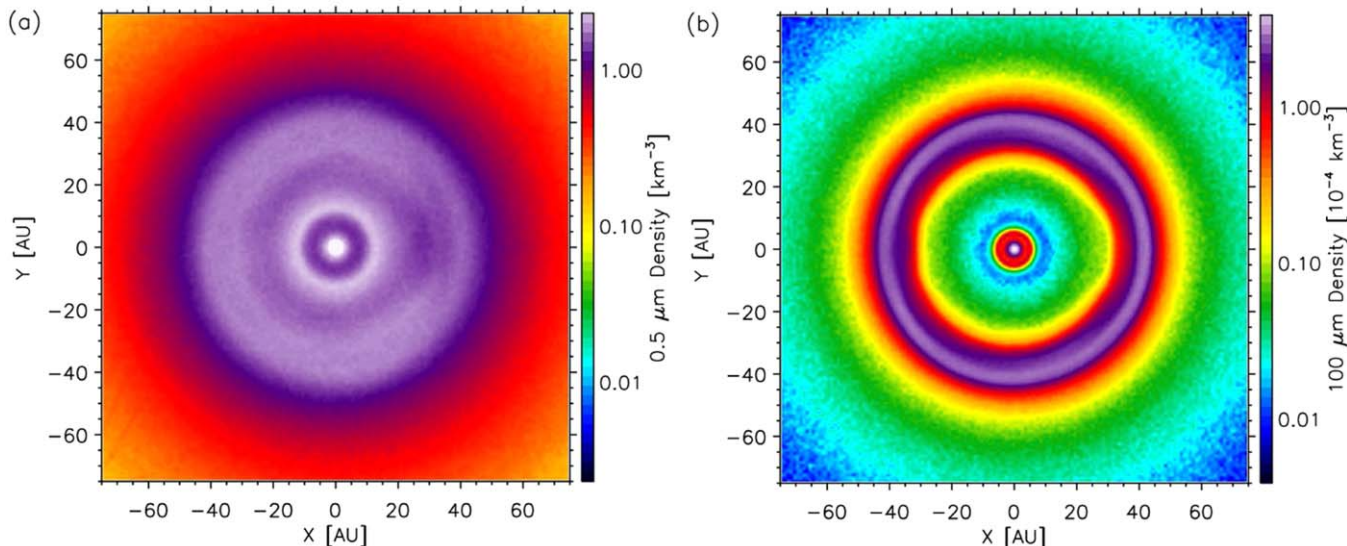


Figure 3. Model for the density distribution of (a) $0.5 \mu\text{m}$ and (b) $100 \mu\text{m}$ interplanetary dust particles in the ecliptic plane based on that presented in Poppe (2016). Though the surface brightness of the light reflected by dust drops as $1/r_S^2$, a density enhancement is expected in the outer solar system near 40 au where LORRI is capable of making measurements in reflection.

(A color version of this figure is available in the online journal.)

planetary satellites (e.g., Verbiscer et al. 2009; Hedman et al. 2009; Poppe & Horányi 2011). An accurate understanding of the size, density, and velocity distributions of IPD throughout the solar system is critical for studies across a broad range of planetary science. The main scientific goal of *New Horizons* remote sensing measurements of the IPD light would be to discern the makeup of the circumsolar dust cloud and its sourcing planetesimals at $r > 45$ au distances. Doing this will help inform comparison of our cloud to the debris disks found around other stars, help us understand the collisions and sublimations of small planetesimals in the outer solar system, and help us understand the exogenous delivery of material of dust from the cloud to solar system bodies (e.g., Earth’s meteors, Pluto’s Haze).

Our knowledge of the IPD distribution in the inner solar system is fairly robust, with recent model-data comparisons concluding that a significant fraction of the IPD particle distribution near 1 au originates from dust emission from Jupiter-family comets with minor contributions from asteroidal and Oort Cloud cometary dust (Nesvorný et al. 2011). The three-dimensional morphology of the inner solar system IPD particle distribution has been mapped in detail via infrared, optical, and spectroscopic imaging (e.g., Liou et al. 1995; Hahn et al. 2002; Ipatov et al. 2008). In contrast, knowledge of the IPD particle distribution in the outer solar system is much more limited. In situ measurements of outer solar system IPD densities have been taken by spacecraft such as *Pioneer* 10 and 11 (Humes 1980), *Ulysses* (Grün et al. 1995a), *Galileo* (Grün et al. 1995b), *Cassini* (Altobelli et al. 2007),

Voyager 1 and 2 (Gurnett et al. 1997), and the *New Horizons* Student Dust Counter (Poppe et al. 2010; Szalay et al. 2013). Despite producing valuable results, these measurements have only provided information on grains with radii between $\sim 0.5\text{--}10 \mu\text{m}$, whereas the peak in the IPD mass flux is expected to be near $\sim 100\text{--}200 \mu\text{m}$. IPD spatial distributions are believed to be a strong function of grain size; for example, Figure 3 shows the $0.5 \mu\text{m}$ and $100 \mu\text{m}$ IPD density (including contributions from Jupiter-family comets, Oort Cloud comets, and EKB objects) from recent modeling efforts (Poppe 2016). Furthermore, since the *Voyagers* have significant out-of-ecliptic trajectories and *Pioneer* 10/11 meteoroid detectors ceased operating inside Uranus’ orbit, only the *New Horizons* Student Dust Counter (Horányi et al. 2008) has probed the EKB region itself, which is the primary source of IPD particles in the outer solar system (e.g., Stern 1996; Liou et al. 1996; Vitense et al. 2010, 2012; Poppe 2016). Finally, model-data comparisons have constrained the overall production rate of dust from the EKB and other cometary sources (Han et al. 2011; Poppe 2016); however, these limits are only based on measurements of grains $0.5\text{--}10 \mu\text{m}$ in radius and are uncertain within an order of magnitude. We require additional observations and/or constraints on the density of IPD in the outer solar system, especially those that address grains with radii from 10 to several hundred μm .

Instruments on the *New Horizons* spacecraft provide a potentially powerful but previously unexplored method of observing the IPD particle density in the outer solar system. Solar light scattered from IPD grains can be observed by *New*

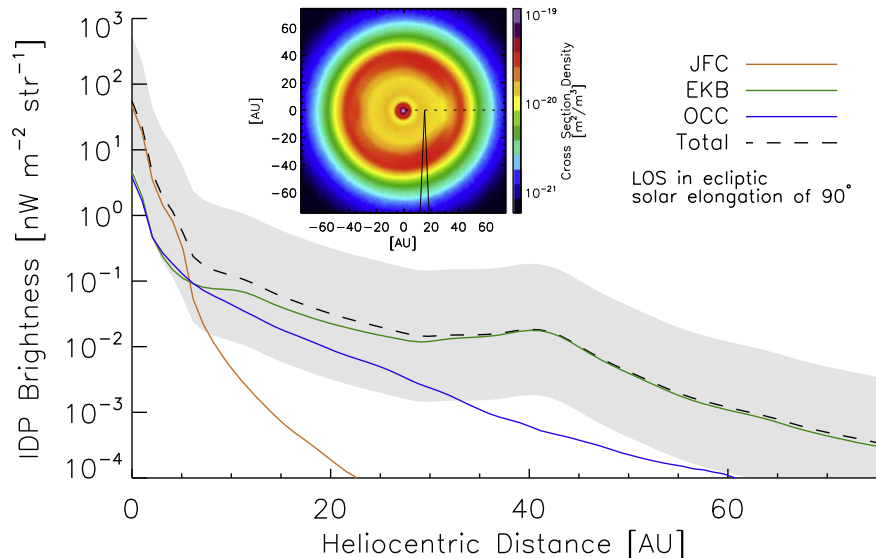


Figure 4. Estimated IPD surface brightness in λ_λ as a function of heliocentric distance for an observer along a radially outward trajectory with solar elongation angle of 90° . Inset: the IPD cross sectional density (m^2/m^3) along with the notional observer.

(A color version of this figure is available in the online journal.)

Horizons as a diffuse background and, in combination with appropriate models for the dust density distribution and light scattering characteristics, can be used to place limits on the IPD distribution. To estimate the brightness scattered from the IPD distribution in the outer solar system, we have used the IPD model of Poppe (2016) which provides three-dimensional IPD densities of Jupiter-family comet, Oort Cloud comet, and EKB dust grains from $0.5\text{--}500\ \mu\text{m}$ with $1\ \text{au} \times 1\ \text{au}$ resolution. We assumed the grains are comprised of astrosilicate material and used appropriate optical constants (Jäger et al. 2003) to compute the scattering phase function from Mie theory. The differential brightness of solar scattered light from each parcel of IPD density over the LORRI wavelength bandpass was summed along the instantaneous line of sight of a virtual observer representing *New Horizons*. Figure 4 shows the predicted IPD brightness in $\text{nW m}^{-2}\ \text{sr}^{-1}$ as a function of heliocentric distance for an observation at a solar elongation angle of 90° (see the inset of Figure 4) along a radially outgoing trajectory (roughly approximating the trajectory of *New Horizons*). In the inner solar system ($r < 5\ \text{au}$), scattered IPD light is on the order of $1\text{--}50\ \text{nW m}^{-2}\ \text{sr}^{-1}$ arising mainly from Jupiter-family comet dust, consistent with *Pioneer 10* photopolarimetry measurements (Hanner et al. 1974). In the outer solar system, the surface brightness slowly tapers off, averaging approximately $0.01\text{--}1\ \text{nW m}^{-2}\ \text{sr}^{-1}$ mainly from contributions by Oort Cloud cometary dust and EKB dust. Importantly, the uncertainty for these model predictions is large, as denoted by the shaded region in Figure 4. Measurements of the scattered IPD brightness by LORRI outside of $40\ \text{au}$ have the potential to constrain the

contributions from Oort Cloud cometary dust and EKB dust to the outer solar system IPD distribution over the summed range of sizes ($0.5\text{--}500\ \mu\text{m}$), representing a powerful new constraint on the outer solar system dust density.

A previous suggestion of direct detection of light scattering from IPD in the outer solar system comes from work by Chary & Pope (2010), who inferred the possible presence of high albedo ($a \sim 1$), icy dust between $\sim 20\text{--}80\ \text{au}$ based on discrepancies between integrated galaxy light (IGL) and the EBL in the mid-IR. They estimated the IPD brightness at optical wavelengths in the outer solar system to be $\sim 25\ \text{nW m}^{-2}\ \text{sr}^{-1}$, several orders of magnitude higher than predicted by our model. Chary & Pope (2010) theorized that such icy, high albedo dust could be shed from comets at distances far from their perihelia (such activity has been detected in Jupiter-family comets Kelley et al. 2013 and could also apply to Oort Cloud comets). If the IPD brightness in the outer solar system is truly this bright, *New Horizons* will be able to detect it, and this information can be used to add an appropriate icy dust grain composition to the current EKB dust models. Intriguingly, the presence of an icy halo of dust in the outer solar system at unexpectedly high densities may not necessarily conflict with in situ measurements by dust detectors (Humes 1980; Poppe et al. 2010) given that icy grains born in the outer reaches of planetary systems may perhaps migrate outward rather than inwards due to mass loss via photodesorption and/or charged particle sputtering and subsequent ejection via stellar (or solar) radiation pressure (i.e., so-called beta meteoroids; Grigorieva et al. 2007). If *New Horizons* provides evidence for isotropic, icy dust grains, current IPD dynamics

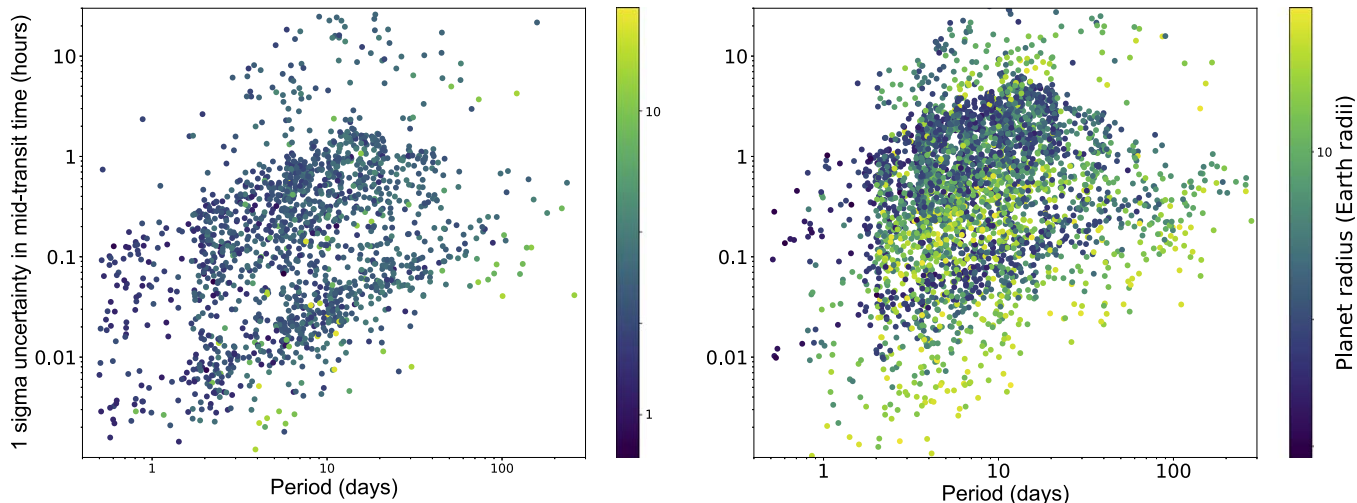


Figure 5. Uncertainty in mid-transit time for simulated planets one year after *TESS* observes them. Left: short cadence (2 minutes). Right: long cadence (30 minutes). (A color version of this figure is available in the online journal.)

models will be revised by adding an additional component of isotropic, icy dust released from Oort Cloud comets and EKB objects.

2.4. Transits in Exoplanetary Systems

Measurements of exoplanet transits can provide a great deal of information about exoplanetary systems (see e.g., Rice 2014 for a review). In the transit method, the light curves of stars hosting exoplanets are photometrically monitored for long periods, and occultations of the star by the planet (or vice versa) are sought. The duration, shape, and repetition frequency of the resulting dip in the star’s light curve can yield a great deal of information about the planetary system. This is the motivation for instruments like *Kepler* (Borucki et al. 2010), which photometrically monitored $>10^5$ stars to search for exoplanets in our galaxy.

Though by now, many thousands of planetary systems have been identified with this method, its promise has only begun to be realized. In addition to wider survey fields, precision photometry could, in principle, allow detection of structures like moons around these planets (Heller 2017). Several methods have been proposed to search for exo-moons, including transit time variations (TTV) and transit duration variations (TDV; see Kipping et al. 2010 for a review), as well as the orbital sampling effect (OSE; Heller 2014). All of these methods rely on both precision photometry of the star, as well as measurements over many orbits of the moon’s parent planet to sample different parts of the moon’s orbital phase. TTVs are also extremely useful for measuring planets masses in systems with multiple transiting exoplanets. These measurements require not only extremely stable photometry, but also that observations occur over a long time baseline to capture the

system in different orbital configurations (Heller et al. 2016a, 2016b).

A vantage point in the outer solar system gives a quiet, stable platform from which to achieve $\delta F/F \sim 10^{-5}$ over the long time baselines required for these measurements. *New Horizons* offers several possible advantages, including (i) the similarity of the LORRI detector with the *Kepler* detectors, which have shown remarkable stability on-orbit (Caldwell et al. 2010); (ii) a well-understood point-spread function, which allows accurate modeling of the instrument response away from the central peak (Morgan et al. 2005; Noble et al. 2009; Cheng et al. 2010); (iii) the lack of ZL variations, giving an extremely stable, systematic-free background in measurements of the same field separated by long periods; and (iv) the quiet instrument environment, in which (presumably) most of the instruments would be in a quiescent state, and e.g., thermal transients from solar heating would be entirely absent.

TESS was successfully launched in 2018 April. During its two-year primary mission, *TESS* will carry out a nearly all-sky survey and is expected to discover thousands of new transiting exoplanets around bright stars. These planets will allow a range of follow-up observations, so in this sense, will be much more valuable than *Kepler* and *K2*. However, due to the photometric precision of *TESS* and the relatively short observing baseline (compared to *K2* or *Kepler*), the ephemerides of most *TESS*-discovered planets will become “stale” very quickly. Figure 5 shows the uncertainty in the mid-transit time of all simulated *TESS* planets with two or more transits, one year after the last transit is observed by *TESS* during the primary mission. Out of approximately 1600 two-minute cadence planets expected from *TESS*, 100 will have 1σ uncertainties on the mid-transit time greater than one hour, and 60 greater than two hours. For the 30-minute cadence, out of 3000 planets, 1000 will have

uncertainties greater than one hour and 500 greater than two hours.

To schedule future observations (new transit photometry for transit timing variation studies, transit and eclipse spectroscopy with the *James Webb Space Telescope (JWST)*, etc.), we will need to recover the ephemerides of these future *TESS* planets. Ground-based resources will not be able to reliably recover transits shallower than $\gtrsim 1$ mmag. Even for deeper transits, recovery of transits from the ground is very challenging if the mid-transit time uncertainties (1σ) are greater than ~ 4 hours, especially when the Earth's diurnal schedule and weather patterns are coupled into the observability window functions. Space-based observatories are needed to avoid ephemeris decay for these planets.

TESS is expected to discover approximately 1000 planets with periods longer than fourteen days that show at least two transits in the *TESS* light curves and have a total signal-to-noise ratio greater than 7.3 (Sullivan et al. 2015). By also exploiting single-transit events, this yield can be increased by 70%, with the potential to discover up to 700 *additional* planets with periods > 14 days. Pursuing single-transit planets can make a large impact particularly at periods longer than 200 days; *TESS* is expected to find just two multiply-transiting planets with period longer than 250 days, with single-transit planets increasing this number by up to an order magnitude (Villanueva et al. 2018).

To confirm those single-transit events that correspond to true planets, the usual vetting process will need to be supplemented with extra steps. One of these steps is to capture a second transit. This will happen after an ephemeris has been obtained using radial velocity (RV) monitoring of the system, and constraints from any additional, multi-transiting planets in the system. However, even with these constraints, the uncertainty on the next mid-transit time will generally be between several hours and several days, making it difficult to ensure a transit is captured from the ground. A space-based observatory such as *New Horizons* could be critical to the confirmation of numerous single-transiting *TESS* planets.

There are currently three existing or near-term space-based observatories that could be used for the long-term monitoring and recovery of transits: *MOST*, *CHAracterising ExOPlanets Satellite (CHEOPS)*, and *Spitzer*. The *MOST* space telescope is not currently funded, and functions only if a user can purchase time. *MOST's* photometric precision is also lower than even that of *TESS* (making it difficult to use for shallower single-transit events), and becomes equivalent to that of ground-based facilities for targets fainter than V mag of 11. The European Space Agency is launching (*CHEOPS*) in early 2019 to obtain optical transits and phase curves of exoplanets. However, large portions of the *TESS* footprint, particularly toward the ecliptic poles, will not be observable by *CHEOPS*. Further, *CHEOPS's* orbit is similar to the *Hubble Space Telescope's (HST)*, meaning that observations will be periodically interrupted by

the Earth so that timing measurements will be more complicated and shorter transit events may be missed. Additionally, the current *CHEOPS* mission lifetime is only 3.5 years. Finally, *Spitzer* is only funded through fall of 2019, so its usefulness for *TESS* follow-up is limited to a few months at most. Even in combination, these three observatories will not be sufficient to monitor the more than 1000 planets with transits shallower than 3 mmag that *TESS* is expected to discover (Sullivan et al. 2015; Barclay et al. 2018).

We note that, while there will likely be a proposal to extend *TESS* past its two-year primary mission, such an extension is far from guaranteed. Even if the mission is approved for a third year extension, the most likely scenario will be to spend the third year reobserving (part of) one of the two ecliptic hemispheres, so we would still need NH for follow-up observations of at least half the *TESS* planets. Further, during an extended mission new planets will be discovered, which will need to be followed up as well (just in time for the potential *New Horizons* astrophysics mission). *New Horizons* would still be a sorely needed resource for observations of additional transits of *TESS*-discovered planets. For the case of single transits, we find that hundreds of single-transit planets will remain unobserved by an extended *TESS* mission (see also Huang et al. 2018, submitted).

To summarize, an extended *New Horizons* mission that can observe *TESS* planet transits throughout the sky could be critical to the rescue of transit ephemerides for future observations, and to the search and confirmation of new *TESS* planets, thus uniquely enhancing the *TESS's* mission science return. We expect NH, in particular the LORRI detector, will be able to reach the photometric precision required to carry out these observations (see Section 4.4.4 for details).

2.5. Discovering Intermediate Mass Black Holes and Breaking Mass Degeneracies in Microlensing

Like exoplanet transits, microlensing of distant stars by foreground massive objects is a time-domain technique wherein photometric monitoring of background stars reveals a distinctive brightening and fading, and where abrupt changes in the light curve can betray the presence of companions to the (normally invisible) lensing body. Typically, stars in our Galaxy's bulge are monitored, as this maximizes the number of potential targets per area on the sky. Microlensing is the most effective method for finding exoplanets beyond the snow line of their stars, where the sensitivity of other planet discovery techniques drops off rapidly. To date, 53 planetary systems detected by microlensing have been published.¹⁵ As the technique does not rely on receiving any light from the lens itself, it is uniquely sensitive to any massive body, including

¹⁵ <https://exoplanetarchive.ipac.caltech.edu>

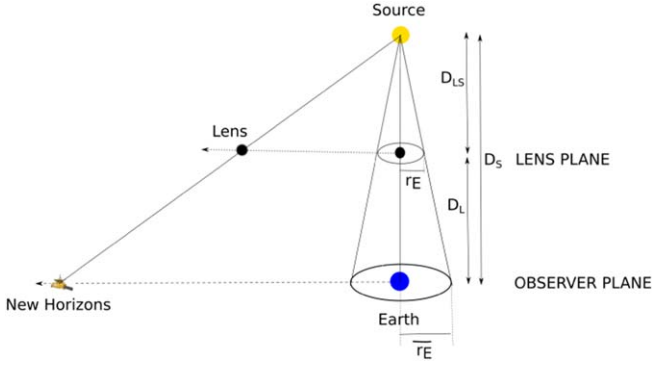


Figure 6. Schematic diagram of the (simplified) geometry of a lensing event as seen from Earth and *New Horizons*, defined such that the Earth-source line is considered to be fixed and the lens moves relative to it. The lensing object is shown as a black dot at the time of maximum magnification as seen from both Earth and *New Horizons*.

(A color version of this figure is available in the online journal.)

compact objects (Wyrzykowski et al. 2011) and even free-floating planets (Mroz et al. 2017).

The mass and distance of a lensing object are degenerate in point source, point lens events, but this can be broken if microlensing parallax can be measured by observing the same event from multiple, widely separated locations (Gould 1992; Buchalter & Kamionkowski 1997). For events with extremely high magnification, the separation required is as small as Earth’s radius (Gould et al. 2009), but these are rare. More commonly, parallax is measured either because the event is long enough for Earth to move in its orbit appreciably during the event (e.g., Muraki et al. 2011), or by obtaining simultaneous light curves from Earth- and space-based observatories such as *Spitzer* and *K2* (e.g., Dong et al. 2007; Yee et al. 2015; Street et al. 2016; Zhu et al. 2017a).

In contrast to those missions, *New Horizons* is now sufficiently distant from Earth that it will only observe a lensing event simultaneously if the lens is massive. A lensing object of mass, M_L , at distance, D_L , from Earth deflects the light of a source at distance, D_S , around itself with a characteristic Einstein radius, $r_E = \sqrt{\frac{4GM_L D}{c^2}}$, where $D = \frac{D_L D_{LS}}{D_S}$ and D_{LS} is the distance between the lens and source (see Figure 6). To give an illustrative example, for a $1 M_\odot$ object at 4 kpc lensing a source at 8 kpc, $r_E = 4.0$ au. Projecting this radius to the plane of the observer (\tilde{r}_E) gives a guide to the region within the solar system from which the event can be seen; any observer within this region will see the object lens the source star at the same time, though the maximum magnification and time of peak will vary as a result of the different closest approach separations observed from different locations. For this stellar-mass lens example, $\tilde{r}_E = 8.1$ au, beyond which the magnification drops off rapidly. The component of *New Horizons*’ separation from Earth perpendicular to the direction of the Galactic Bulge is ~ 11.9 au at time of

writing, placing it outside the projected Einstein radius of a stellar-mass lens, meaning that the magnification it would experience while the event is seen lensed from Earth would be undetectably small.

However, a unique and exciting possibility is to use *New Horizons* to observe lensing by stellar-mass black holes. Compared with the example above, for a $10 M_\odot$ black hole, $\tilde{r}_E = 25.5$ au, which is a good match to *New Horizons*’ future position. A number of theories for the formation of these objects have been proposed including primordial objects formed soon after the Big Bang (Carr et al. 2016) to the remnants of stellar evolution (Elbert et al. 2018), but the difficulties of observing them have made these theories hard to test. Interest in this subject has been renewed as merging binary black holes are one source of the recent detections of gravitational wave events (e.g., Abbott et al. 2016). Microlensing offers a way to measure their masses and binarity and, with an adequate sample, establish a measured mass function which can be compared with predictions.

New Horizons’ extraordinary velocity, currently 14.0 km s^{-1} , is close to half of the average orbital velocity of the Earth ($\sim 30 \text{ km s}^{-1}$). In the course of a typical event lasting ~ 60 days, the spacecraft moves $7.4 \times 10^7 \text{ km}$ or ~ 0.5 au, on a trajectory where the major component of motion is perpendicular to the Galactic plane. By comparison, Earth travels ~ 1 au around its orbit and ~ 0.3 au perpendicular to the Galactic plane within the same time frame. The trajectory of *New Horizons* may produce a significant parallax signature which might be detected from *New Horizons* light curves, even without additional data. It is therefore valuable to explore whether this can be distinguished from degeneracies and used to characterize the events.

Once a lensing event has been seen from Earth, the relative motion of the lens carries it out of alignment with the original observer. In the case of massive ($\sim \text{few } M_\odot$) lenses, the source will still appear magnified from *New Horizons*, with a time offset in the event peak, while the magnification for lower mass lenses will be negligible.

It is worth noting that for a small fraction of stellar-mass lenses, the relative trajectory of the source could in principle subsequently cross the line of sight to the source from *New Horizons*, so that the spacecraft would experience a different lensing event caused by the same lens, after a delay of a few months, for lenses moving with typical relative velocities of $\sim 120 \text{ km s}^{-1}$. A small number of events discovered at one observing platform might therefore be followed up from the other. For events where constraints on parallax can be derived from Earth-bound observations (for instance), one component of the parallax ($\pi_E = AU/\tilde{r}_E = (\pi_{E,N}, \pi_{E,E})$) is typically measured with far greater precision than the other. Nevertheless, if the first observer can place some constraints on the event parallax, this information could be used to pre-select targets most likely to exhibit a lensing event from the second

platform, and those follow-up observations would provide much tighter constraints on the lens trajectory and event model and hence on the lens' physical parameters.

Companion objects in any lensing system can cause light curve anomalies that are most likely to occur if the projected separation of the companion from the primary lens at the time of the event happens to coincide with positions of the images of the source created by the primary lens, close to the Einstein radius. Observations of an event therefore act to probe for companions at specific locations in the plane of the lens, which can be mapped (e.g., Tsapras et al. 2016). Naturally, during the delay between the peak of events caused by the same lens as seen from both Earth and *New Horizons*, any companion objects move in their orbits around the primary lens. Observations of a second lensing event therefore effectively probes more of the lens plane, improving our sensitivity to lens companions. These could also be used to detect binary source stars, as their orbit would subtly change their lens-source-observer alignment between events, and hence affect the observed magnification.

The probability of microlensing occurring is intrinsically low, but highest in the direction of the dense star fields of the Galactic bulge (e.g., the rate for stellar-mass lensing is $\Gamma = 4.60 \pm 0.25 \times 10^{-5} \text{ star}^{-1} \text{ yr}^{-1}$ at $|b| \sim -1.4$ and $2.25 < l < 3.75$ for sources with $I < 20$, see Sumi & Penny 2016). Microlensing programs therefore necessarily observe in highly crowded fields, and require reasonably high spatial resolution instruments. For this reason, *New Horizons'* LORRI telescope is best suited to this science.

LORRI offers a spatial resolution of 1×1 arcsec and a single wide optical passband. While its pixel scale is somewhat larger than current ground-based optical surveys (e.g., OGLE has 0.26 arcsec/pixel resolution) it is comparable with some of the telescopes used by ground-based follow-up teams (e.g., MicroFUN¹⁶). The larger pixel scale means that the lensed source will suffer somewhat higher blending with nearby stars, but this can be determined by modeling the event light curve provided it is sampled at a range of different magnifications. LORRI's wide passband is beneficial to harvesting as much light as possible from the relatively faint source stars ($I < 20$ mag) and the photometric precision required for microlensing is relaxed compared with transit measurements, typically $\sim 1\%$. Its reasonably wide field of view, which is similar to that of the first-generation microlensing surveys, could be used to monitor multiple events at once.

In addition to a well-sampled light curve, multi-band photometry is required to determine the spectral type and distance of the source star in a microlensing event. For massive lenses, this could be obtained from facilities on Earth, but for stellar-mass lenses, the Ralph-MVIC instrument offers five passbands through the optical that could be used for this

purpose, though with lower spatial resolution. While non-optimal in these crowded fields, this resolution is similar to that of *Kepler*, which has provided light curves of microlensing events thanks to advanced detrending techniques (Zhu et al. 2017b). Ralph-MVIC has a brighter limiting magnitude than LORRI ($R = 15.3$ mag at current maximum integration time), owing to its smaller aperture, and an asymmetric field of view. This instrument is therefore better suited to a more targeted strategy, obtaining low-cadence multi-band imaging of selected bright events during their peaks.

While the rate of black hole lensing is not well established, we can estimate the number of stellar-mass lensing events which *New Horizons* could detect from the distribution of baseline source star magnitudes alerted each year by the ground-based surveys. Of 1834 events found by OGLE in 2017, 824 (44.9%) had a baseline (i.e., unlensed) magnitude $I < 18.6$ mag, LORRI's limiting magnitude in a 30s integration. Of these, 46 events had a baseline brighter than Ralph-MVIC's limiting magnitude. This figure underestimates the number of events which could be observable to Ralph-MVIC however, as color observations are primarily required over the peak of an event when the target is brighter. While ground-based surveys cover a footprint that is much larger than *New Horizons* could monitor, they have also shown that events are not uniformly distributed across the Bulge (Poleski 2016); $\sim 41\%$ are discovered within a central $\sim 3.3 \times 3.3^\circ$ region.

The most compelling case for microlensing with *New Horizons* would be a targeted strategy toward selected events discovered from Earth then observed at low cadence (once every few days/weeks) from the spacecraft, minimizing the downlink overheads (see Section 4.4.5 for details). This cadence would be sufficient to properly constrain the light curves of massive lenses.

2.6. Transient Follow-up

The study of astronomical transients touches on many areas of physics. The explosions of massive stars as supernovae reveal the physics of matter under intense densities and temperatures, and provide insights into shock physics, the origins of the elements, and the sources of extragalactic neutrinos, high-energy particles, and gamma-rays. Rapid follow-up of gravitational wave detections has only begun, but the discovery of the first kilonova is already shedding light on the neutron star equation of state, the physics of their mergers, and the resulting r -process nucleosynthesis and its role in producing the heavy elements.

Many of these phenomena occur with timescales ranging from a few days to a few months. Occasionally, critical phases of these events, or even entire events, could be missed due to the relative positions of Earth, the Sun, and the event being studied. One notable example is the recent electromagnetic counterpart to the gravitational wave event GW170817

¹⁶ <http://www.astronomy.ohio-state.edu/~microfun/>

(Abbott et al. 2017a, 2017b), which has allowed us to constrain the ejecta properties and the associated nucleosynthesis, study the environment of the neutron star merger, and for the first time, use gravitational wave events as “standard sirens” (Abbott et al. 2017c), providing a completely new probe for cosmology. Had GW170817 occurred just one week later, it would have been unobservable to Earth-based ultraviolet, optical, and infrared telescopes due to Sun constraints, so the electromagnetic counterpart would not have been found, and the incredible insights (e.g., Metzger 2017, and references therein) gained from this event would have been lost.

More events need to be observed to settle the disputed nature of some of the emission components, and to improve the uncertainties in the inferred cosmological parameters. The expected rate of binary neutron star merger detections is uncertain, due to both order-of-magnitude uncertainties in the intrinsic rates of such mergers and uncertainties in the final sensitivity of the LIGO and Virgo detectors. However, when LIGO and Virgo reach design sensitivity, the event rate could be between a few per year and a few per week (Abbott et al. 2017a). Because LIGO and Virgo are not sensitive to Earth’s position relative to the Sun and can detect gravitational waves from any position in the sky, a large fraction of these events will be unobservable to any optical, ultraviolet or infrared telescope in existence, except one far from Earth. For approximately half of the year, *New Horizons* is opposite the Sun from Earth, and therefore has exclusive access to large parts of the sky.

Even a single detection by *New Horizons* could make the difference between identifying a counterpart candidate and not identifying one, which in itself is an important constraint on the physics of the event. In addition, this would localize the host galaxy, potentially setting interesting constraints on merger environments and hence populations (e.g., Blanchard et al. 2017; Pan et al. 2017), and allowing a (later) redshift determination for cosmological measurements (e.g., Abbott et al. 2017c). In addition, a well-timed data point could help constrain the rise, peak or decline emission properties of a kilonova, each of which is critical for discerning competing emission models (e.g., Arcavi 2018 and references therein).

Several of the instruments that found the electromagnetic counterpart to GW170817 have very similar properties to those of LORRI. Despite the small field of view of LORRI compared with the LIGO and Virgo localization regions (of tens of square degrees), the counterpart was quickly identified by pointing telescopes to a list of known galaxies in the localization region (Nissanke et al. 2013; Singer et al. 2016; Gehrels et al. 2016; Arcavi et al. 2017a). This same strategy could be used with *New Horizons* when gravitational waves from a binary neutron star, or neutron star black hole merger, are detected on the opposite side of the Sun from Earth. Even though the data could not be transmitted to us immediately, detecting the counterpart in retrospect, and obtaining even a single flux

measurement, would be extremely useful for many of the above science cases.

Additionally, *New Horizons* could be used to follow events discovered close to their observability limit, such as was the case with GW170817. In this scenario, the counterpart would be identified by other telescopes, and *New Horizons* would be used to image it once it can no longer be observed from Earth or Earth orbit. The point source sensitivity of LORRI is adequate to detect the kilonova associated with GW170817 that peaked at $r \sim 17$ (Arcavi et al. 2017b; Drout et al. 2017; Pian et al. 2017; Valenti et al. 2017). The GW170817 kilonova faded rapidly, and would have been below the LORRI detection limit within a few days. Also, had it been more distant, it might have been below the LORRI detection limit for the entire flare. However, it is still not clear how typical the GW170817 kilonova is, and whether future events may have a different peak magnitude and fading timescale.

Additional high-value and time-critical transients could also be observed by *New Horizons*. Even single-epoch flux measurements of particular supernovae can be critical in bridging observing gaps due to Sun constraints. For example, the nearest superluminous supernova to date, SN 2017egm, became unobservable due to Sun constraints just 2–3 weeks after peak brightness (e.g., Nicholl et al. 2017; Bose et al. 2018). At a *V*-band magnitude of ~ 15 it would have been readily observable by *New Horizons*. The physical mechanisms responsible for powering superluminous supernovae are still debated (e.g., Howell 2017), and even a handful of observations would have been extremely useful to track the light curve over the 2.5 months until it became observable again, constraining its post-peak decline, and informing emission models. There are a handful of similar events each year where *New Horizons* could fill in such gaps in the data.

3. Sensitivity and Stability Estimates

To determine the capability of *New Horizons* for astrophysical observations, it is necessary to estimate the sensitivity of the instrument to both unresolved and resolved emission. In Table 1, we summarize the parameters of LORRI, Ralph, and Alice based on published pre-launch and in-flight assessments of their performance (Morgan et al. 2005; Conard et al. 2005; Weaver et al. 2008; Cheng et al. 2008; Reuter et al. 2008; Stern et al. 2008; Noble et al. 2009; Cheng et al. 2010; Zemcov et al. 2017). Based on these parameters, we can derive simple point source and extended emission sensitivities that take into account the instrument performance (Bock et al. 2013).

The surface brightness sensitivity estimate for LORRI listed in Table 1 is based on in-flight performance that the *New Horizons* team has measured. Zemcov et al. (2017) performed a detailed study of the LORRI performance in the context of astrophysical observations of diffuse surface brightness, and find performance figures in agreement with the LORRI team. In

Table 1
A Summary of the Characteristics of New Horizons Instruments Capable of Astrophysical Observations

Parameter	LORRI	Ralph-MVIC	Ralph-LEISA	ALICE
Instrument type	Single-band imager	Multi-band imager	Imaging spectrometer	Spectrometer
Wavelength range ⁱ	440–870 nm	400–975 nm	1.25–2.5 μm	470–1880 \AA
Spectral resolution	1.2	1.2 (pan & framing), 3.2 (blue), 3.9 (red), 4.5 (IR), 17.7 (CH4)	240	133
Spatial resolution (arcsec ²)	1.0×1.0 (or 4.1×4.1) ⁱ	4.1×4.1	12.8×12.8	1000×1000
Number of pixels	1024×1024 (or 256×256) ⁱⁱ	Framing channel 5024×128 ; all others 5024×32	256×256 (~ 1 pixel per spectral element)	1024×32
Field of view (sq. deg.)	0.29×0.29	5.7×0.037	0.9×0.9	$0.1 \times 4.0 + 2.0 \times 2.0$
Telescope primary aperture (cm)	20.8	7.5	7.5	4×4
Point-spread function FWHM (arcsec)	2	6	19	...
Data size (Mb frame ⁻¹)	16 (or 1 ⁱⁱ)	17.9	1.0	0.5
Maximum integration time (s)	30	10	4	3600 ⁱⁱⁱ
Point source sensitivity ⁱ	$V = 20.5$ in 4×4 pixel bins ⁱⁱ for <i>G</i> -type star	$R = 15.3$	$J = 10.6, H = 9.8, K = 8.9$...
Per-pixel surface brightness sensitivity ^{iv}	$2.2 \times 10^3 \text{ nW m}^{-2} \text{ sr}^{-1}$	$3.8 \times 10^4 \text{ nW m}^{-2} \text{ sr}^{-1}$	$6.0 \times 10^4 \text{ nW m}^{-2} \text{ sr}^{-1}$	0.4 Rayleigh
Characteristic surface brightness sensitivity ^{iv}	$10 \text{ nW m}^{-2} \text{ sr}^{-1}$	$95 \text{ nW m}^{-2} \text{ sr}^{-1}$	$750 \text{ nW m}^{-2} \text{ sr}^{-1}$ in $R = 10$ bins	$0.4 \text{ nW m}^{-2} \text{ sr}^{-1}$ at $R = 133$

Notes.

ⁱ Approximate performance; please see Stern et al. (2008) and references therein for details.

ⁱⁱ Deep observations are typically performed in 4×4 pixel binning mode to improve sensitivity.

ⁱⁱⁱ The maximum programmable integration time is actually 65,535 s, but 3600 s is typically considered the functional maximum.

^{iv} $1\sigma \lambda_\lambda$ at maximum integration time (as discussed in Section 4.3). Red channel specifications listed for MVIC.

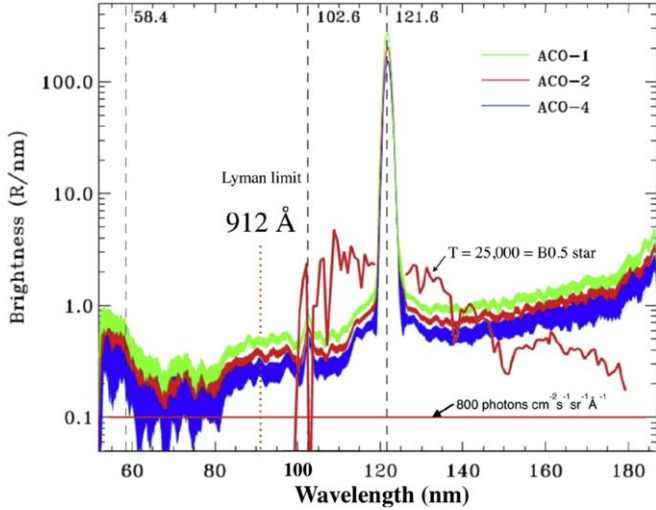


Figure 7. Three published Alice spectra of the interplanetary medium, showing the decline in surface brightness with increasing heliocentric distance observed in the same field (Gladstone et al. 2013). Also appearing is the spectrum of a hot star, with a vertical scale exaggerated by a factor 1.5 to bring out more clearly the stellar spectral features that we hope to detect (or, more dramatically, to fail to detect) in Alice observations of the cosmic background. A brightness of 0.1 R/nm corresponds to 0.01 R/Å or 800 photons $\text{cm}^{-2} \text{s}^{-1} \text{Å}^{-1}$. These spectra are dominated by the light of solar Ly α scattering off the interstellar hydrogen that is constantly flowing through the solar system. As *New Horizons* becomes more distant, this foreground component decreases, as is apparent from these observations that were made many months apart. (A color version of this figure is available in the online journal.)

that work, the quoted calibration factors are referenced to a flat-spectrum source, but there is no tension between them and recent calibration work with *New Horizons*.

The sensitivity characteristics of Alice are given in Stern et al. (2008) and summarized in Figure 7. The instrumental Ly α foreground has been declining steadily, and recent unpublished Alice observations show that the instrument is currently at a level such that we can expect to obtain spectra with astrophysical as opposed to instrumental information in coming years (Murthy, private communication).

MVIC is well characterized, and has observed a variety of astronomical objects during cruise phase (Olkin et al. 2006; Howett et al. 2017). As a result, its noise properties and radiometric calibration are quite well understood, and are summarized in Table 1. As a check of the predictions given in Reuter et al. (2008), we performed an analysis of the 2006 observations of Asteroid 2002 JF56, and found array standard deviations well matched to the notional noise levels in calibrated data. As predicted, the effective surface brightness sensitivity is worse than that for LORRI, largely due to the combination of smaller aperture, narrower spectral bandpass, and shorter maximum integration time.

To assess the sensitivity of LEISA, we have studied data taken on the star Vega (α Lyr) in late 2008. In this observation,

the star was scanned across the dispersive direction of the imaging array with $t_{\text{int}} = 0.59$ s per resolution element. The total observation time was 198 s. The data are calibrated to I_{λ} in $\text{erg s}^{-1} \text{cm}^{-2} \text{sr}^{-1} \text{Å}^{-1}$ using the nominal calibration factor for LEISA (derived, in part, from these same data). In our analysis, we performed aperture photometry of the star image in each frame, using a circular aperture of $r = 2$ pixels and an outer annular aperture of $2 < r < 4$ pixels. We then subtract the *HST* CALSPEC Flux Standard for α Lyr and compute the standard deviation of the residuals (Bohlin 2014) to determine $\sigma(I_{\lambda})$. From this, we estimate $\sigma(\lambda I_{\lambda})$ to be $< 6.7 \times 10^4 \text{ nW m}^{-2} \text{sr}^{-1}$ per pixel in a 4 s integration and assuming the FWHM of the beam is $1.44 \times$ the pixel resolution (Reuter et al. 2008), which is consistent with the published estimate of $6.0 \times 10^4 \text{ nW m}^{-2} \text{sr}^{-1}$ per pixel.

The instrument most useful for exoplanet investigations is LORRI, where the primary parameter of interest is the photometric stability of the instrument. To help assess the photometric stability of LORRI, we have used data from the Pluto cruise phase of the *New Horizons* mission centered on $(\alpha_{J2000}, \delta_{J2000}) = (18^{\text{h}}02^{\text{m}}06, -14^{\circ}37'8)$. This field happened to be the position of Pluto as viewed from *New Horizons* between 2012 and 2014 while the mission was in-bound from about the orbit of Uranus. Pluto was still a faint object in these images, and many stars are visible in them. An example image is shown in Figure 8.

The data discussed here were reduced and calibrated using the pipeline described in Zemcov et al. (2017). As in that work, these observations are “found data” that are not ideal for this type of stability characterization, but they do provide an estimate sufficient for our purposes. The data records consist of 191 $t_{\text{int}} = 10$ s integrations on the Pluto monitoring field taken from June 2012 to July 2014. Following calibration, for each field we find $R_L > 13.1$ sources and perform photometry on them using SEXTRACTOR in AUTO_MAG mode. We cross-identify the sources over images using their positions, and reject $R_L < 11.3$ sources as they saturate the detector in this integration time. Because the field is near the Galactic plane, they suffer from source crowding, giving us a wide sampling of environments. Also, the position angle and pointing of the images shifts over the course of the observation epoch, so a particular source is not always present in a given image. Figure 9 summarizes the photometry measurements for a selection of 20 relatively bright sources over the course of the observations. Importantly, we see no evidence for turn-on effects after ~ 1 year of hibernation, meaning that observations separated by long time intervals do not seem to suffer from transient effects related to power cycling.

To summarize the photometric performance of LORRI, we compute the median absolute deviation (MAD) of the flux measurements for each source. We perform this calculation for the full set of 191 observations taken over two years, and for a subset of the data taken in 2013 July. The subset consists of three blocks of contiguous observations, each consisting of

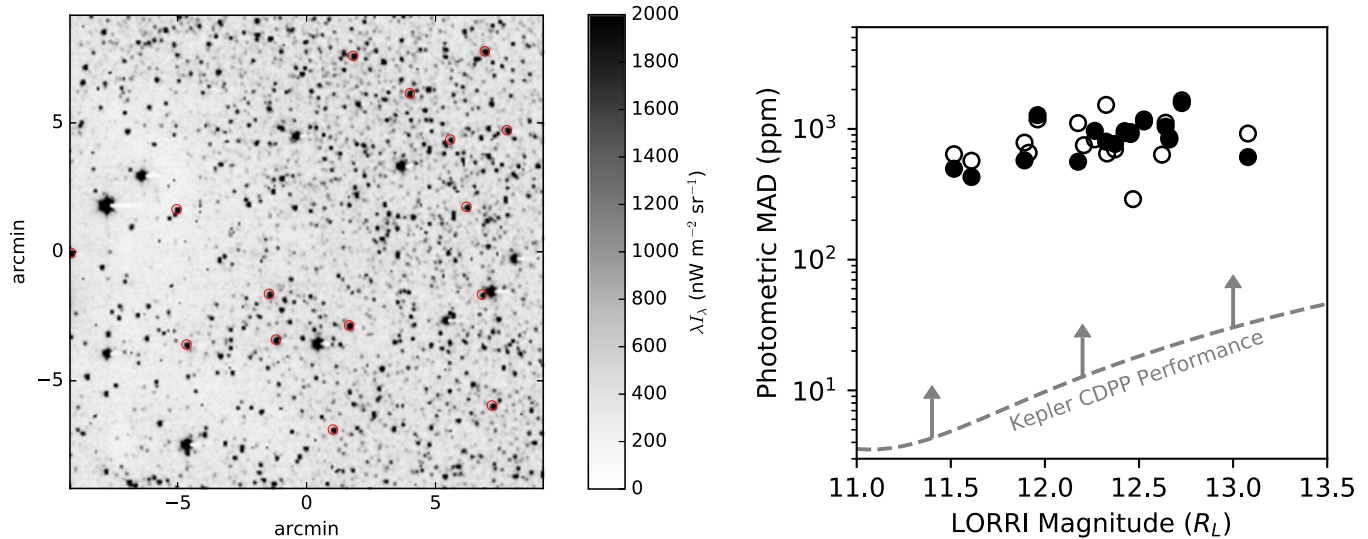


Figure 8. Left panel: an example image of the photometry stability field we study in this work. The image is calibrated as λ_λ . Stars selected for the photometry study described here are circled, and lie within $13.1 < R_L < 11.3$. Some of the stars used in the study do not fall into this image, but do fall in others in the set of observations. Right panel: an assessment of the photometric precision of LORRI based on 191 $t_{\text{int}} = 10$ s observations acquired from summer 2012 to summer 2014 (open circles), and 87 observations over a 5.5 hour period from July 2013 (filled circles). Both populations are expressed as parts per million in flux. This measurement is not ideal, as we do not have access to six hours of continuous 10 s integrations, but compare our results to the lower limit from the *Kepler* mission, which (in “long integration” mode) is more than an order of magnitude more stable at these source fluxes. That difference in performance can be accounted for by the different aperture size, integration time, pointing control, and data analysis between these observations and *Kepler*’s.

(A color version of this figure is available in the online journal.)

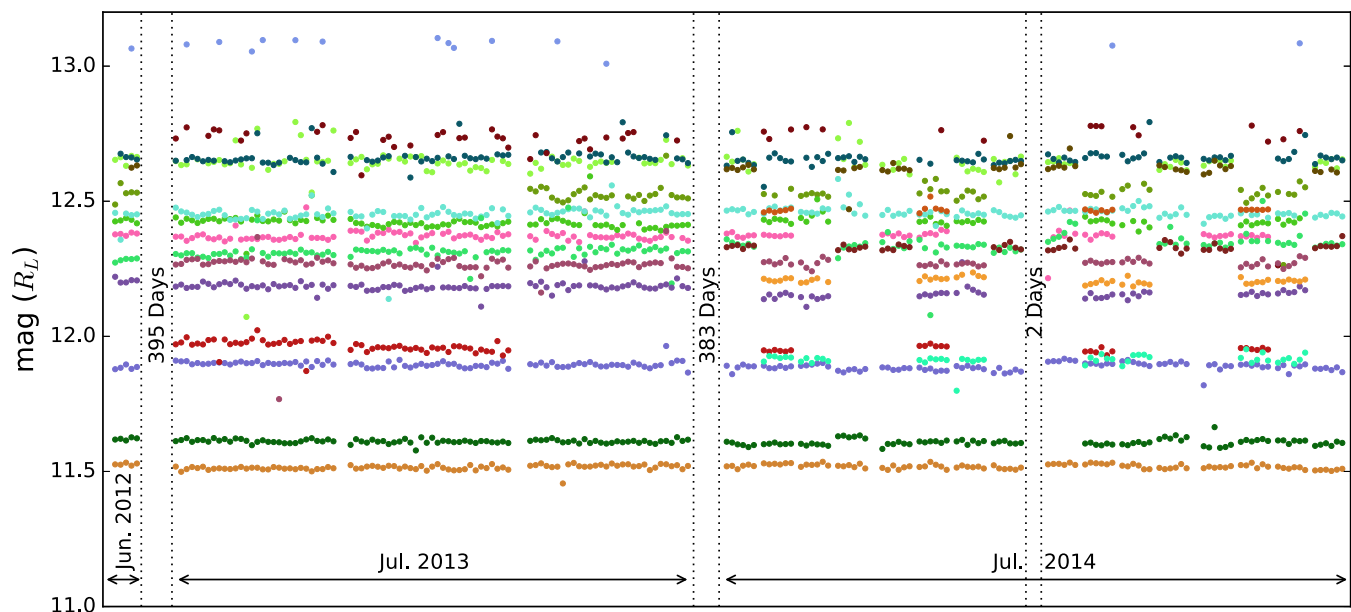


Figure 9. Measured fluxes of sources over three major observation epochs on the same field acquired between 2012 June and 2014 July. The time axis has been compressed to aid visualization; gaps between points are roughly logarithmic, with the shortest corresponding to tens of seconds and the longest corresponding to hundreds of days. The largest temporal discontinuities are highlighted by vertical dashed lines. Because of the changing central position and position angle of the images with time, a given source may or may not be visible in a particular observation. The variations in these photometric data are used to calculate the photometric precision shown in Figure 8, particularly the data set taken in 2013 July, which covers about 5.5 hours. We find no evidence for effects related to waking the instrument after year-long hibernations, and find the stability of the detector is excellent over the period.

(A color version of this figure is available in the online journal.)

29×10 s integrations, each spread about 2.5 hours apart. This subset constrains the behavior of the photometry over a ~ 6 hour period, which can be compared against six-hour accuracy measurements for other instruments in the literature.

The MAD results scaled to ppm of flux for the ensemble are summarized in Figure 8. For reference, we compare this to *Kepler*'s "long integration" photometric accuracy (Jenkins et al. 2010; Gilliland et al. 2011; Christiansen et al. 2012; Vanderburg & Johnson 2014). We find the LORRI photometric stability is 1–2 orders of magnitude less accurate at these magnitudes. This estimate does not probe the photometric precision continuously over the six-hour period during which complex effects we would be unaware of can begin to have an effect, and if these are present they could inflate the variance in the data. Though not the most accurate conceivable instrument, we conclude that LORRI is capable of precise enough photometry to do interesting science.

4. Considerations for Survey Operations

Though the astrophysical science possible from *New Horizons* is compelling, there are practical considerations that limit the observations possible with the spacecraft. There are both programmatic and technical complications that would need to be addressed before *New Horizons* could be used for these observations. In addition to the costs associated with data telemetry, keeping the operations team active, etc., these observations may impose extra stress on the spacecraft that could result in additional risk to the mission.

In this section, we discuss these technical limitations, their impacts on the science cases, and present a hypothetical operations scenario that would generate a rich and unique data set. Our predictions are based on publicly available information, and we note that a detailed engineering study of the observations fully considering the spacecraft subsystem performance is beyond the scope of the current work. Properly designed, the new insights these observations would lead to are unlikely to be rivaled for the foreseeable future.

4.1. Attitude Control Considerations

Due to power considerations, *New Horizons* does not have a reaction wheel-based pointing system. Instead, hydrazine thrusters are used to provide pointing control. Attitude data from the star tracker and a laser-ring gyroscope system are input to a feedback loop to set the pointing within prescribed limits in both absolute astrometry and drift. In three-axis mode, a targeted position can be found to within $1/2$ (1σ), and active scans can be controlled to that location within a typical deadband of $1/7$. The nominal passive drift rate once an attitude has been achieved is $5''\text{s}^{-1}$ (Conard et al. 2017), though analysis of images suggests it is frequently significantly better (Zemcov et al. 2017). Details of the attitude control

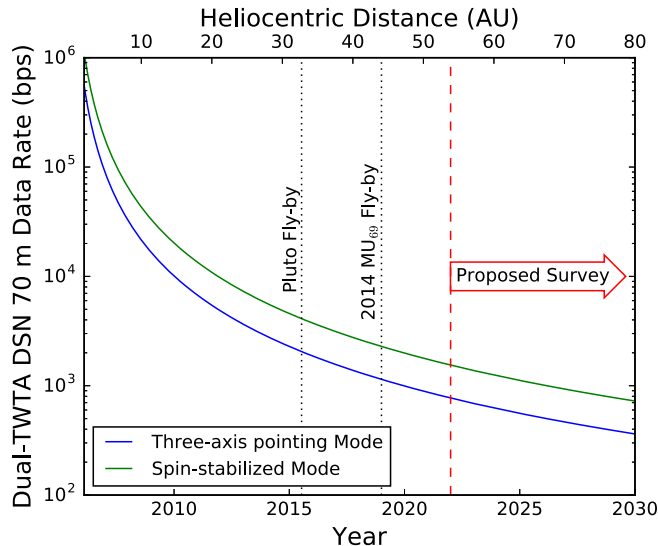


Figure 10. Data downlink rate from *New Horizons* vs. time and heliocentric distance. The maximum achievable rate given in bits per second (bps) decreases as R_{\odot}^{-2} and depends on the attitude control mode of the spacecraft. In this calculation we assume the DSN 70 m dish is used in Dual-TWTA mode (see Fountain et al. 2008 for details).

(A color version of this figure is available in the online journal.)

system can be found in Rogers et al. (2006) and Fountain et al. (2008).

In addition to the attitude control performance, the propellant required to point the spacecraft is a limiting factor to the observations performed during any extended mission. At this time, the predicted mass of propellant following the end of the KEM mission is 10 kg, as compared with about 40 kg remaining at the end of the primary Pluto fly-by mission (Bushman 2017). As a benchmark, a change in *New Horizons*' spin rate of 5 RPM (the change from the nominal spin rate to zero RPM for three-axis control mode) requires approximately 0.125 kg of hydrazine (Fountain et al. 2008). Ultimately, the remaining propellant is likely to be the limiting factor in determining precisely which observations and science cases are possible in an extended mission for astrophysics.

4.2. Telemetry Considerations

Downlinking data from distant instruments has presented a challenge since the beginning of deep-space missions. As an example, the data acquired for the prime *New Horizons* Pluto fly-by mission required only one week to acquire, but over 16 months to telemeter back to Earth. The available bandwidth only decreases with time as the distance to *New Horizons* increases. In Figure 10, we show the achievable data rate from the beginning of the *New Horizons* mission until 2030, at which point the spacecraft will be some 80 au from us (Fountain et al. 2008).

Assuming the proposed astronomical measurements do not occur until 2022 following the 2014 MU₆₉ extended mission, we expect a maximum data rate in three-axis pointing mode (i.e., the mode in which observations will be performed) to be ~ 900 bits per second (bps). If observational data were telemetered in spin-stabilized mode this increases to ~ 1.8 kbps. The per-frame size of the various *New Horizons* data products is given in Table 1, and typically measure in the ~ 10 Mb range. Assuming a 50% duty cycle and 30% compression, even at maximum telemetry speed this corresponds to only 240 Mb per day, which is approximately 120 mins of LORRI data, or 15 mins of MVIC/LEISA integrations.

4.3. Other Instrument Limitations

In addition to attitude control and telemetry, there are additional constraints on the instrument hardware to consider. The first of these is the maximum allowable integration time for the instruments, which was set to 30 s for LORRI (Cheng et al. 2008), 10 s for MVIC, and 4 s for LEISA (Reuter et al. 2008) at launch. Alice’s maximum integration time of 18 hrs is less restrictive, though long-term pointing drifts may prove problematic here. For flux-limited observations, because of the low data downlink rate, it is desirable to increase the integration time to achieve equal sensitivity in fewer detector reads. However, because of *New Horizons*’ relatively poor attitude control performance, longer integrations may suffer from image smearing as source images track along the detector. Given typical attitude drift rates, integrations lasting several minutes might offer an advantage. Such changes are feasible; the *New Horizons* team is in the process of increasing LORRI’s maximum integration time to 60 s (H. Weaver, 2017, private communication). Optimizing integration times requires a detailed trade study to understand the benefits and costs given the constrained attitude control, telemetry rate, and particulars of a science case, which we leave to future work.

A second consideration is the optical performance of the instruments. LORRI’s rejection of off-axis light is relatively poor, such that viewing within a solar elongation angle of 90° results in scattered light in the image (Cheng et al. 2010). Further, there are optical ghost paths between $0^\circ 2'$ and $0^\circ 35'$ from the optical axis, which leave out-of-focus images of the secondary mirror on the detector array (Cheng et al. 2010). In addition, LEISA suffers from a solar light leak with rays sensed by the detector coming from behind the instrument at the 10^{-7} level (Reuter et al. 2008). Though it is not difficult to work within these restrictions, some science cases (for example, imaging toward the inner solar system) are precluded. Other optical features that must be considered in the design of observations requiring high sensitivity and stability may also be present; this is another issue that requires detailed communication with the instrument teams to optimize.

4.4. Assessment of Science Cases

Given the instrument sensitivities and practical considerations discussed above, here we assess the feasibility of the different science cases presented in Section 2. The sky available for observations covers the 2π sr away from the Sun, which contains the $\Delta\ell = 180^\circ$ around the Galactic center, as well as a variety of extragalactic deep fields for EBL measurements. There are no power limitations nor spacecraft maneuvering constraints associated with pointing the instruments away from the line of sight to Earth.

4.4.1. Measurement of EBL

Of the *New Horizons* instruments, the most sensitive instrument to diffuse emission is LORRI, which has the largest telescope aperture and widest bandpass. The expected IGL at LORRI’s wavelength is ~ 8 nW m⁻² sr⁻¹. As a result, if no pixel masking were required and only uncorrelated random noise were present, it should be possible to measure the IGL at $S/N \gtrsim 0.5$ in a single 30 s integration with LORRI. However, it is necessary to mask some fraction of pixels that contain bright stars, and the actual noise in the instrument is not ideal. As a result, the previous measurement (Zemcov et al. 2017) reached a statistical error of 7 nW m⁻² sr⁻¹ in 240 s of integration time. To reach an uncertainty level comparable to the current uncertainty on IGL in a single field, some 400×30 s integrations would be required. In Table 2 we give estimates of the total number of integrations and total observation time required for this measurement (assuming no overheads), as well as an estimate of the time required to telemeter the data. Assuming a best telemetry rate of 900 bps, 30% data compression ratio, and 50% duty cycle, this data set would require 1.6 days to transmit to Earth. Though more time-consuming than the actual observations by a factor of 600, this is a relatively inexpensive measurement. Statistical sensitivity is not likely to limit this measurement as the CCD dark current stability, astrophysical foregrounds, and other effects would be relatively large at these low flux levels. The observation design would therefore rest on acquiring adequate knowledge of the system performance and foregrounds to be confident in the measurement.

With a pixel rms of $>4 \times 10^4$ nW m⁻² sr⁻¹ in 10 s, MVIC would require $\sim 10^3$ integrations to reach a statistically significant EBL measurement, which in turn would require a few hours to execute. Information from all five MVIC channels would be telemetered at once, providing low-resolution spectral information in the optical, which is an important addition to a LORRI measurement. However, the data telemetry for MVIC becomes a real consideration, with the transmission time for this data set estimated to be a significant fraction of a year. MVIC does have dark (i.e., non-illuminated) pixels to allow a measurement of the detector current in the absence of photons

Table 2
Surface Brightness Sensitivity Targets and Requirements.

Instrument	Target Sensitivity ($\text{nW m}^{-2} \text{sr}^{-1}$, 1σ)	Number of Integrations Required ^a	Integration Time Required	Time to Telemeter ^b
LORRI	1	400	200 min	1.6 days
MVIC	2.5	1,500	240 min	100 days
LEISA (+10% SIM ^c)	5 (at $R = 10$)	25,000	27 hrs	95 days

Notes.

^a Assumes maximum programmable integration time.

^b Assumes a data rate of 900 bps, 30% compression ratio, and 50% data transmission duty cycle.

^c Assumes “Solar Illumination” mode (SIM) is used to monitor the dark current every 10 observations.

(Reuter et al. 2008), an important prerequisite to absolute photometric measurements (Matsuura et al. 2017).

Finally, LEISA would provide a unique measurement of the EBL, as it covers crucial infrared bands where observations of the emission from early galaxies are possible. LEISA’s sensitivity is poor, and it would require at least two days equivalent observation time to execute observations that would yield a $\sim 3\sigma$ detection of the EBL per $R = 10$ band. However, we again encounter a situation where the data telemetry is time-consuming, largely due to the number of 4 s integrations required to achieve a useful surface brightness sensitivity. Though LEISA does not have built-in dark pixels, the instrument can be used in “Solar Illumination” mode where a small pick-off mirror assembly couples only $\sim 3,000$ pixels to external illumination (Reuter et al. 2008). A suitable choice of standard mode observations interspersed with Solar Illumination mode observations can offer close to real-time assessment of the dark current in the PICNIC detector array.

It is likely that the dominant foreground after star masking will be the DGL. This signal follows the structure of the Milky Way, and can be slightly fainter than the EBL, but is never zero. As a result, a typical approach to subtracting the DGL component from the isotropic EBL is to observe a number of fields and correlate against a template for the DGL emission, usually based on maps of thermal emission from dust in the ISM. The extrapolation to $I_{\text{DGL}} = 0$ then provides an estimate for the EBL component. To demonstrate the isotropy of the measured EBL, it is necessary to repeat this process in several independent field sets at various ecliptic and galactic latitudes. For the LORRI observations this would multiply the single-field estimates by the number of fields to be observed, however, the per-field observation time could be reduced because the error on the EBL would be dominated by the overall fit uncertainties rather than the absolute uncertainty in a single field. A precise optimization of the observations depends on details we leave for the future, but it is likely that an order of magnitude more LORRI observations than indicated above would allow us to demonstrate isotropy of the signal. This type of measurement is prohibitively expensive for the Ralph

measurements, but we could reasonably rely on isotropy demonstrated by LORRI alone.

4.4.2. Ultraviolet Background Sensitivity

The nominal sensitivity of Alice is $\sim 1R$ per pixel at $R = 133$ over a 32 kpixel detector array in a 600 s integration. Averaging over pixels, we estimate a total background sensitivity of about 0.02 R/nm in this integration time, which corresponds to approximately 1,600 photons $\text{cm}^{-2} \text{s}^{-1} \text{sr}^{-1} \text{\AA}^{-1}$. Current estimates for the UV background place its surface brightness at < 100 photons $\text{cm}^{-2} \text{s}^{-1} \text{sr}^{-1} \text{\AA}^{-1}$, meaning that we would require 256 integrations to reach an interesting sensitivity limit (Henry et al. 2015). However, the UV background is faint compared to the galactic foregrounds, so Alice is expected to yield interesting new information in only 30 integrations. Because Alice observations are relatively inexpensive to telemeter, we would be able to both execute the observations and telemeter the resulting data in an equal amount of time. For 256 observations, we estimate 2 days of observation and 2 days of telemetry are required. This observation is inexpensive enough that many fields could be targeted on the sky, as long as propellant costs did not become problematic.

4.4.3. EKB Dust Observations

The primary regions of interest for IPD light scattering will be those centered on the ecliptic where the IPD particle density is highest, but also away from the galactic background, where DGL will contaminate the images. Though the very lowest levels of modeled IPD surface brightness would be too challenging to reach with LORRI, deep $< 1 \text{ nW m}^{-2} \text{sr}^{-1}$ sensitivities remain a real possibility, and would allow us to constrain models for the composition and structure of the EKB. The example calculation of IPD brightness shown in Figure 4 assumes silicate grains; however, we can also input other dust grain compositions including ice mantle/silicate cores, carbonaceous, and organic compositions (e.g., Warren 1984; Jenniskens 1993; Quinten et al. 2002; Jäger et al. 2003). The observations would likely be performed as a function of solar elongation, and repeated over time as the sight line through the

dust cloud changed to help deconvolve the structure profile. One interesting possibility to boost the signal is to measure the EKB analog to the Gegenschein, which is due to reflection of sunlight from dust in the directly anti-solar direction that boosts the surface brightness of the local ZL signal by factors ~ 100 . Unfortunately, the anti-solar direction for *New Horizons* lies not far from the Galactic plane $\{\ell, b\} = (16^\circ, -14^\circ)$, so the galactic backgrounds may be large. However, even upper limits to the EKB dust surface brightness would be unique and useful in this regard. We would estimate that ~ 10 positions at different solar elongations, observed every 5 au in heliocentric radius, would make an excellent data set requiring only two months to telemeter.

4.4.4. Exoplanet Transits

Exoplanet transits are typically studied in relatively bright star systems, and require photometric accuracy better than 1:1000 over ~ 1 hour timescales for studies of anomalous features in the light curve. For a $V = 8$ star, we would require a 1σ photometric accuracy of $\delta V = 15.5$ to detect the presence of the planet around e.g., HD209458, which is significantly above LORRI's $t_{\text{int}} = 30$ s sensitivity. This bodes well for the use of LORRI in observing transits. We do not suggest that LORRI would be appropriate for finding transiting systems, but rather that it could be used to follow up particularly interesting targets with known (or well-constrained) ephemerides.

Due to the need for propellant, it would be far too expensive to operate LORRI in a constant-monitoring mode as was done with e.g., *Kepler*. A more efficient use of the finite resources would be to target known transiting systems to better characterize them. Both the transit timing and transit duration methods require precise measurements of a planet's light curve over many transits to build up a model of transit timing variations for mass measurements, or of a possible moon's orbit. The quiet environment and diagnostic information about the detector would be very useful in ensuring instrument stability of this time. However, LORRI will mostly be used to improve the transit parameters and the uncertainty on the ephemerides of known transiting exoplanets (including those to be discovered by *TESS*). All of these observations rely on well-understood and low-error light curves, which *New Horizons* is in a unique position to generate.

In terms of operations, the data requirement of, for example, a 30 s observation every five minutes for two hours would generate only 24 frames for telemetry. The requirement of pointing stability would be more problematic, as would the active pointing required to keep the source in the same pixels over time, since this requires active use of propellant. This expenditure would have to be traded in the context of the larger mission goals and observations.

4.4.5. Microlensing

Microlensing events can magnify a source star by up to several magnitudes over the course of events lasting between ~ 1 day to several months. Single-lens events can be detected with relatively low-cadence imaging, where the frequency required is a function of the Einstein timescale, t_E , and hence proportional to the lens mass. A sampling rate of once every 0.5–3 days is needed to detect stellar-mass lenses while black hole lens events require imaging only once every 1–2 weeks. However, both stellar and planetary *binary* events that comprise $\sim 10\%$ of the total are characterized by short-lived (\sim hours—days) light curve anomalies which must be sufficiently well sampled to constrain the model. Typical observations aim for a photometric precision of < 0.01 mag, and a cadence of at least four per hours $^{-1}$. We consider the practical implications of several possible observing strategies.

LORRI's wide field of view suggests a survey strategy where *New Horizons* would repeatedly image the region of highest microlensing rate over the course of > 2 months. The overall length of the observations would be determined by the need to measure the lensing light curve both over the peak of the event and at unlensed baseline to properly constrain the event magnification and timescale. Surveying the full $\sim 3^\circ \times 3^\circ$ central Bulge region would require a 11×11 mosaic of LORRI images. Although in principle it could achieve a cadence of ~ 4 hrs, this strategy would be prohibitively expensive on propellant. Furthermore, it would accumulate data far in excess of the downlink capacity, some ~ 11.9 GB/day (noting that bulge observations could not be binned to preserve spatial resolution). Surveying four LORRI field pointings once a day (or conversely, one field every 6 hrs) has a more practical data rate of 67.2 MB day $^{-1}$. The wider footprint would ensure more events are detected (~ 22 year $^{-1}$ versus ~ 5 year $^{-1}$), while a single pointing would conserve propellant. Arguably the most practical survey strategy would be to image as large a footprint as possible at a cadence of \sim once per week for a total duration of > 150 d, with the goal of detecting black hole lenses. Concurrent observations of the same footprint conducted from Earth could be used to measure the event parallax and determine the physical properties of the lenses. However, it is difficult to estimate the yield of black holes detected this way as the rate is not well known.

A second possible strategy would take advantage of *New Horizons*' unique position to act as an "early warning system." As noted above, some fraction of events observed by *New Horizons* may subsequently be observed from Earth in separate lensing events after a delay of ~ 0.5 yr. Were the spacecraft to undertake a very wide angle, but low- (~ 1 –3 day) cadence survey of a wide region, there would be sufficient time to downlink the data and discover events which could then be intensively followed up from Earth and near-Earth missions.

LORRI could survey a 4×4 grid of pointings, $\sim 1^\circ.16 \times 1^\circ.16$ each, once every 3 days with a data rate of 89.6 MB day^{-1} .

The final (and probably most practical) option would be the converse: to use *New Horizons* to follow-up selected events discovered from Earth and/or by *WFIRST*. Events observed from both Earth and *WFIRST* will already have constraints on the lens-source relative trajectory, allowing more stringent target selection, and many will already be known to have planetary or binary signatures. In this way, *New Horizons* could act as a “force multiplier” for those surveys, to search for other planetary or stellar companions in the same systems thanks to its distinct line of sight to the event. This strategy would require higher cadence observations (ideally $< 1 \text{ hr}$) but over a shorter period during the peak of the event, with lower cadence (every $\sim 3 \text{ days}$) observations taken before and after the peak to measure the event magnification. As an example, a similar measurement with from EPOXI used only 20 observations over the course of 48 hours to break degeneracies in the system MOA-2009-BLG-266 (Muraki et al. 2011). This suggests the characterization of a single system could require only tens of observations, which would require much less than a day to downlink.

4.4.6. Transient Follow-up

LORRI has the point source sensitivity to reach the flux of some transient sources, and is stable over long time periods. Measurement of transient events would require a “fast track” observation upload scheme. It is likely that at least several days would pass between the detection of an event and a *New Horizons* observation taking place, and data would not necessarily be telemetered immediately. Further, these measurements would only be useful for the period when *New Horizons* is near the Sun as viewed from the Earth and observation from the ground is impossible. It would be advantageous to optimize the *New Horizons* observation epochs to coincide with these periods, so that the instrument would already be in a mode to execute astrophysical observations. This requirement may not be compatible with rapid command uplink using the high-gain antenna. As a result of these additional requirements, the use of *New Horizons* for transient measurements remains somewhat speculative at this point.

4.5. A Hypothetical Observational Campaign

In designing an observational campaign, there are three major factors to consider: (i) the time required to telemeter the data back to Earth, and the storage capacity and reliability of the onboard data volumes; (ii) the need to expend fuel for observations requiring active pointing control; and (iii) optical and communications restrictions on the attitude of the spacecraft.

As shown in Table 2, the time to telemeter the data can easily grow to be prohibitive. The most cost-efficient instrument in terms of sensitivity per data volume is LORRI, and we assume that most of the observations would be performed with it. Even so, the data storage considerations impose a survey design similar to the *New Horizons*’ planetary encounters, where an observation campaign is pre-programmed and executed contiguously, and then later telemetered to Earth while the spacecraft is in spin-stabilized mode. This scheme takes advantage of the downlink rate boost of spin-stabilized mode. Based on purely data telemetry considerations, we therefore propose a scheme where observations are performed roughly annually in a short burst, and then telemetered during a cruise phase. This pattern could be repeated for a number of years, and would ultimately be limited by the fuel required to maneuver the spacecraft.

The attitude control system likely limits the lifetime of the mission. To conserve the resource, observations that would not require active pointing control, or at least could be performed with periodic pointing correction, would be preferable. Assuming the nominal post-acquisition drift rate of $5'' \text{ sec}^{-1}$, a target centered on the LORRI detector array would drift off the field of view in > 1.7 minutes. This sets a natural cadence for attitude correction during measurements of point sources that minimizes fuel consumption. For deep observations of diffuse surface brightness, and even more conservative viewing mode would be to point the telescope on target, and then let it drift for some specified time before re-pointing. For observations of emission that varies smoothly over sub-degree scales (for example, EBL, DGL, or IPD light), the spacecraft could wander for up to one hour, by which time the center of the field of view would have drifted by $0^\circ.5$. Point source emission could easily be masked following the post facto image registration, and foreground emission requiring image-space correlation could just use the reconstructed pointing of each image separately. The most challenging measurements are those requiring photometric precision, where drift causes a source to wander between pixels that have different relative photo-response. These observations are likely to require tighter attitude control than studies of diffuse brightness. However, if controlled, in this work we have shown that LORRI can perform adequately to allow unique observations of both exoplanet transits and microlensing.

The third consideration in our survey design are attitude constraints due to the instruments, communications, or other features of the spacecraft. One obvious constraint is for the imaging instruments to have a solar elongation $> 90^\circ$ at all times during an observation, which constrains the field of regard to $2\pi \text{ sr}$ away from the Sun, which will be close to frozen in celestial coordinates for the duration of the mission. There are almost certainly additional constraints for the high-gain antenna and other systems, and for keeping the solar

illumination of the spacecraft roughly constant to minimize thermal disturbances.

All of these constraints considered, *New Horizons* is still capable of generating a rich and unique data set for astrophysical science. For the EBL science case, we would measure 5–10 independent fields with LORRI to $\pm 1 \text{ nW m}^{-2} \text{ sr}^{-1}$ to show isotropy in the signal, and at least one field to $\pm 3 \text{ nW m}^{-2} \text{ sr}^{-1}$ error with MVIC and $\pm 4 \text{ nW m}^{-2} \text{ sr}^{-1}$ error with LEISA. These measurements would require a large number of integrations added together, likely acquired over different epochs.

A measurement of the UV background with Alice is quite tractable, and requires only of order days of integration and telemetry time to achieve interesting sensitivities that cannot be reached from vantage points near the Earth. The scientific goals of our proposed Alice observations are served well by any and all observations of any regions of the sky. Particularly valuable will be comparison of Alice spectra obtained while pointed toward regions at high galactic latitudes compared against the same at low galactic latitudes (where starlight scattered from dust is expected to dominate the spectra, demonstrating instrumental capability). Valuable data will be obtained on any target that is observed in pointed mode, and the pointing stability can drift considerably without harm to the value of the data obtained. To conserve propellant and aid in cross-correlation studies, it is likely that the UV measurements would be performed concurrently with and on the same fields as the EBL measurements. Obviously, it would be necessary to develop a detailed observation plan that would optimize the observation strategy.

For the EKB dust measurement, we would measure ~ 10 fields placed at different ecliptic latitudes in each epoch of a multi-year mission. Because the EKB dust is spatially smooth, these observations would not require tight pointing control. Measuring to $\pm 1 \text{ nW m}^{-2} \text{ sr}^{-1}$ error with LORRI in each epoch would allow a detailed probe of the structure of the EKB. Spectral information from MVIC and LEISA is likely too expensive to be considered, but the EBL measurements may permit interesting constraints on the longer wavelength behavior of the EKB dust emission. It is likely these fields and the extragalactic background fields would be designed in a coordinated fashion, since the observational requirements are very similar.

In our envisioned survey we would also observe a subset of known transiting systems to improve the ephemerides, and monitor transit timing variations if there are multiple transiting planets. The subset of systems to be observed would be selected based on prioritization of targets for atmospheric characterization with the *JWST* and large ground-based telescopes. These observations require pointing on a particular target for long periods of time (hours to days) with observations at a relatively fast cadence (~ 10 per hour), so would be expensive in terms of propellant. Assuming a 2-day measurement with a 5 minute cadence of 30 s LORRI

observations, we would require 576 frames to be telemetered. Potentially, $\gtrsim 10$ such observations could be carried out in a year.

Traditional exoplanet microlensing measurements require close to constant monitoring of fields in the Galactic bulge region to increase the number of possible targets. A microlensing survey based on this design would thus require fairly constant sampling of a single target field for as long a baseline as possible, and active pointing correction to keep the field of view on target. Here, we envision a different approach. An Earth-based microlensing survey monitoring a known field could have a real-time event pipeline that triggers on suspected star-star lensing events. During *New Horizons* observation campaigns, these triggers could be passed to the science team and programmed into the queue with priority. The ~ 10 day duration of these events gives ample time to design and upload an observation into the queue. The light curve of the source would be monitored for several days, and short-duration microlensing events indicative of exoplanets could be sought.

Science cases that require point source photometry would benefit from windowing the image to a region around the target of interest, as this would significantly reduce the telemetry bandwidth requirement. At the other extreme, onboard co-addition of images could allow an increase in the signal-to-noise ratio of static sources of emission. Both algorithms would have to take into account the absolute pointing accuracy of the instrument and the drift of the images over time. Finally, to maximize the available fuel resources, observations would need to be designed to minimize slew distances on the sky. Since observations are planned well in advance (except for microlensing events), this is not a prohibitive requirement. Following a ~ 1 week long observation campaign each year, *New Horizons* would go into spin-stabilized mode and begin transmitting the data to Earth.

4.6. The Possibility of Science Observations During Spin-stabilized Operations

Given the limited propellant budget for pointed observations, one possibility of interest is to perform astrophysical observations in some form of the spin-stabilized operation. This would provide the benefit of increasing the data telemetry rate while allowing different parts of the sky to be surveyed by the instruments. The primary drawback of this scheme is related to the detectors; all of the detectors on the *New Horizons* instrument suite suitable for astrophysical observations are of the charge integrating type, which usually require stable pointing over the course of an integration to provide clean images of the sky. The cost of having *New Horizons* spin during observations is that the astrophysical signal would be smeared over multiple pixels, thereby complicating image analysis and, in the limit of read-noise limited measurements,

decreasing the total signal-to-noise ratio on the source. For a purely isotropic signal, or one that is not spatially structured on the angular scale of the spin smear, this is not problematic. However, most of the science cases discussed here require spatial resolution either to monitor a point-like source, or to remove it through masking. As a result, allowing the spacecraft to spin could be problematic.

In *New Horizons*' standard spin-stabilized mode the spacecraft is spinning around the high-gain antenna's boresight at 5 RPM, which corresponds to $30^\circ \text{ minute}^{-1}$. This is clearly prohibitively fast, as it means (for example) that LORRI's field of view is moving one full array width every 0.6 s. Even in unreasonably short integration times, images of stars would be smeared. As a conservative estimate for the preferred spin rate, we impose the requirement that, over a full 30 s integration, the LORRI image can shift by 0.5 pixels, or 2 arcsec. This corresponds to a spin rate of 3.1×10^{-6} RPM, which is clearly a different engineering regime than the current spin-stabilized mode. Due to their larger pixels and shorter integration times, the other instruments could accept relatively faster spin rates, though still within an order of magnitude of the LORRI requirement. Faster spin rates may also be acceptable, with a concomitant loss in scientific capability. This kind of observation may be enabling for EBL science with MVIC and LEISA, where the required integration times and data volumes are probably prohibitive in pointed mode, but if the observations can be spread over many months they become more tractable.

We conclude that, though it may be technically challenging to implement, it is worth studying the possibility of a spin-stabilized mode with a very slow spin rate. Observing in this mode would not require any propellant, would increase the data telemetry rate, and would allow maps of large areas of sky to be constructed. Some of the science cases, particularly those related to diffuse emission, could potentially benefit from such an observation strategy.

5. Conclusions

With a fully functioning *New Horizons* beyond the orbit of Pluto, the astrophysical and planetary communities have a rare opportunity to perform unique science with an instrumentation suite capable of deep and precise observation of the cosmos. In this paper we have motivated the broad scientific fields such observations can address, as well as studied the performance of the instruments and discussed the various limitations and considerations a future survey with *New Horizons* would have to address. We find that *New Horizons* is well suited to astrophysical observation, and that a carefully designed survey optimizing the expenditure of propellant and telemetry bandwidth while minimizing spacecraft operational risk could provide interesting new insights in astrophysics. Some data of astrophysical interest is already available in the archive, and the

analysis of these is ongoing. Insights from these will help us design better observations. Going forward, we suggest a study of the detailed feasibility of astrophysical observations with *New Horizons* combining the *New Horizons* instrument and engineering teams with astrophysical experts in the various scientific fields discussed here. This will permit an accurate assessment of the current capabilities of the instruments and spacecraft and a detailed observation plan to be formulated.

We thank the *New Horizons* science and instrument teams for their decades of dedicated effort designing, building and flying such a complex mission, and in particular H. Weaver for his patience in answering our largely impenetrable queries and his thoughtful input on our work. We would also like to thank B. Crill for his insightful comments that helped improve the study, and our six referees for their incisive thoughts.

The *New Horizons* cruise phase data sets used in this work were obtained from the Planetary Data System (PDS). Support for I.A. was provided by NASA through the Einstein Fellowship Program, grant PF6-170148. A.R.P. was supported by the NASA Planetary Atmospheres program, grant #NNX13AG55G. D.D. acknowledges support provided by NASA through Hubble Fellowship grant HSTHF2-51372.001-A awarded by the Space Telescope Science Institute.

ORCID iDs

Michael Zemcov,  <https://orcid.org/0000-0001-8253-1451>

References

- Abbott, B. P., Abbott, R., Abbott, T. D., et al. 2016, *ApJL*, **833**, L1
 Abbott, B. P., Abbott, R., Abbott, T. D., et al. 2017a, *PhRvL*, **119**, 161101
 Abbott, B. P., Abbott, R., Abbott, T. D., et al. 2017b, *ApJL*, **848**, L12
 Abbott, B. P., Abbott, R., Abbott, T. D., et al. 2017c, *Natur*, **551**, 85
 Akshaya, M. S., Murthy, J., Ravichandran, S., Henry, R. C., & Overduin, J. 2018, *ApJ*, **858**, 101
 Altobelli, N., Dikarev, V., Kempf, S., et al. 2007, *JGR*, **112**
 Arcavi, I. 2018, *ApJL*, **855**, L23
 Arcavi, I., McCully, C., Hosseinzadeh, G., et al. 2017a, *ApJL*, **848**, L33
 Arcavi, I., Hosseinzadeh, G., Howell, D. A., et al. 2017b, *Natur*, **551**, 64
 Barclay, T., Pepper, J., & Quintana, E. V. 2018, arXiv:1804.05050
 Bernstein, R. A. 2007, *ApJ*, **666**, 663
 Blanchard, P. K., Berger, E., Fong, W., et al. 2017, *ApJL*, **848**, L22
 Bock, J., Beichman, C., Cooray, A., et al. 2012, SPIE Newsroom, doi:10.1117/2.1201202.004144
 Bock, J., Sullivan, I., Arai, T., et al. 2013, *ApJS*, **207**, 32
 Bohlin, R. C. 2014, *AJ*, **147**, 127
 Borucki, W. J., Koch, D., Basri, G., et al. 2010, *Sci*, **327**, 977
 Bose, S., Dong, S., Pastorello, A., et al. 2018, *ApJ*, **853**, 57
 Bowyer, S. 1991, *ARA&A*, **29**, 59
 Broadfoot, A. L., Sandel, B. R., Shemansky, D. E., et al. 1977, *SSRv*, **21**, 183
 Buchalter, A., & Kamionkowski, M. 1997, *ApJ*, **482**, 782
 Burns, J. A., Lamy, P. L., & Soter, S. 1979, *Icar*, **40**, 1
 Bushman, S. S. 2017, Performance of the New Horizons Propulsion System through the Pluto Encounter (American Institute of Aeronautics and Astronautics), <https://doi.org/10.2514/6.2017-4746>
 Caldwell, D. A., Kolodziejczak, J. J., Van Cleve, J. E., et al. 2010, *ApJL*, **713**, L92
 Cambrésy, L., Reach, W. T., Beichman, C. A., & Jarrett, T. H. 2001, *ApJ*, **555**, 563

- Carr, B., Kühnel, F., & Sandstad, M. 2016, *PhRvD*, **94**, 083504
- Chary, R.-R., & Pope, A. 2010, arXiv:1003.1731v1
- Cheng, A. F., Conard, S. J., Weaver, H. A., Morgan, F., & Noble, M. 2010, *Proc. SPIE*, **7731**, 77311A
- Cheng, A. F., Weaver, H. A., Conard, S. J., et al. 2008, *SSRv*, **140**, 189
- Christiansen, J. L., Jenkins, J. M., Caldwell, D. A., et al. 2012, *PASP*, **124**, 1279
- Christon, S. P., Hamilton, D. C., Plane, J. M. C., et al. 2015, *JGRA*, **120**, 2720
- Conard, S. J., Weaver, H. A., Núñez, J. I., et al. 2017, *Proc. SPIE*, **10401**, 104010W
- Conard, S. J., Azad, F., Boldt, J. D., et al. 2005, *Proc. SPIE*, **5906**, 407
- Cooray, A. 2016, *RSOS*, **3**, 150555
- Cooray, A., Bock, J. J., Keatin, B., Lange, A. E., & Matsumoto, T. 2004, *ApJ*, **606**, 611
- Cooray, A., Amblard, A., Beichman, C., et al. 2009, *Ast*, 2010 astro2010: The Astronomy and Astrophysics Decadal Survey
- Cuzzi, J. N., & Estrada, P. R. 1998, *Icar*, **132**, 1
- Dixon, W. V. D., Sankrit, R., & Otte, B. 2006, *ApJ*, **647**, 328
- Dong, S., Udalski, A., Gould, A., et al. 2007, *ApJ*, **664**, 862
- Drout, M. R., Piro, A. L., Shappee, B. J., et al. 2017, arXiv:1710.05443
- Durisen, R. H., Cramer, N. L., Murphy, B. W., et al. 1989, *Icar*, **80**, 136
- Edelstein, J., Bowyer, S., & Lampton, M. 2000, *ApJ*, **539**, 187
- Elbert, O. D., Bullock, J. S., & Kaplinghat, M. 2018, *MNRAS*, **473**, 1186
- Estrada, P. R., Durisen, R. H., Cuzzi, J. N., & Morgan, D. A. 2015, *Icar*, **252**, 415
- Feuchtgruber, H., Lellouch, E., de Graauw, T., et al. 1997, *Natur*, **389**, 159
- Fountain, G. H., Kusnierkiewicz, D. Y., Hersman, C. B., et al. 2008, *SSRv*, **140**, 23
- Frankland, V. L., James, A. D., Carrillo-Sánchez, J. D., et al. 2016, *Icar*, **278**, 88
- Gehrels, N., Cannizzo, J. K., Kanner, J., et al. 2016, *ApJ*, **820**, 136
- Gilliland, R. L., Chaplin, W. J., Dunham, E. W., et al. 2011, *ApJS*, **197**, 6
- Gladstone, G. R., Stern, S. A., & Pryor, W. R. 2013, in *New Horizons Cruise Observations of Ly α Emissions from the Interplanetary Medium*, ed. E. Quémerais, M. Snow, & R.-M. Bonnet (New York: Gladstone), 177
- Gong, Y., Cooray, A., Mitchell-Wynne, K., et al. 2016, *ApJ*, **825**, 104
- Gordon, K. D., Witt, A. N., & Friedmann, B. C. 1998, *ApJ*, **498**, 522
- Gorjian, V., Wright, E. L., & Chary, R. R. 2000, *ApJ*, **536**, 550
- Gould, A. 1992, *ApJ*, **392**, 442
- Gould, A., Udalski, A., Monard, B., et al. 2009, *ApJL*, **698**, L147
- Grigorieva, A., Thébault, P., Artymowicz, P., & Brandeker, A. 2007, *A&A*, **475**, 755
- Grün, E., Baguhl, M., Divine, N., et al. 1995a, *P&SS*, **43**, 971
- Grün, E., Baguhl, M., Divine, N., et al. 1995b, *P&SS*, **43**, 953
- Gurnett, D. A., Ansher, J. A., Kurth, W. S., & Granroth, L. J. 1997, *PhRvL*, **24**, 3125
- Gustafson, B. A. S. 1994, *AREPS*, **22**, 553
- Hahn, J. M., Zook, H. A., Cooper, B., & Sunkara, B. 2002, *Icar*, **158**, 360
- Hamden, E. T., Schiminovich, D., & Seibert, M. 2013, *ApJ*, **779**, 180
- Han, D., Poppe, A. R., Piquette, M., Grün, E., & Horányi, M. 2011, *GeoRL*, **38**, L24102
- Hanner, M. S., Weinberg, J. L., DeShields, L. M., II, Green, B. A., & Toller, G. N. 1974, *JGR*, **79**, 3671
- Hauser, M. G., & Dwek, E. 2001, *ARA&A*, **39**, 249
- Hedman, M. M., Murray, C. D., Cooper, N. J., et al. 2009, *Icar*, **199**, 378
- Heller, R. 2014, *ApJ*, **787**, 14
- Heller, R. 2017, arXiv:1701.04706
- Heller, R., Hippke, M., & Jackson, B. 2016a, *ApJ*, **820**, 88
- Heller, R., Hippke, M., Placek, B., Angerhausen, D., & Agol, E. 2016b, *A&A*, **591**, A67
- Henry, R., Murthy, J., & Overduin, J. 2018, arXiv:1805.09658
- Henry, R. C. 1991, *ARA&A*, **29**, 89
- Henry, R. C., Murthy, J., Overduin, J., & Tyler, J. 2015, *ApJ*, **798**, 14
- H.E.S.S. Collaboration, Abramowski, A., Acero, F., et al. 2013, *A&A*, **550**, A4
- Holberg, J. B. 1986, *ApJ*, **311**, 969
- Holberg, J. B., & Barber, H. B. 1985, *ApJ*, **292**, 16
- Horányi, M., Hoxie, V., James, D., et al. 2008, *SSRv*, **140**, 387
- Howell, D. A. 2017, in *Superluminous Supernovae*, ed. A. W. Alsabti & P. Murdin (New York: Springer AG)
- Howett, C. J. A., Parker, A. H., Olkin, C. B., et al. 2017, *Icar*, **287**, 140
- Huang, C. X., Shporer, A., Dragomir, D., et al. 2018, *AJ*, submitted (arXiv:1807.11129)
- Humes, D. H. 1980, *JGR*, **85**, 5841
- Hunter, J. D. 2007, *CSE*, **9**, 90
- Ipatov, S. I., Kutyrev, A. S., Madsen, G. J., et al. 2008, *Icar*, **194**, 769
- Jäger, C., Dorschner, J., Mutschke, H., Posch, T., & Henning, T. 2003, *A&A*, **408**, 193
- Jenkins, J. M., Caldwell, D. A., Chandrasekaran, H., et al. 2010, *ApJL*, **713**, L120
- Jenniskens, P. 1993, *A&A*, **274**, 653
- Jones, E., Oliphant, T., Peterson, P., et al. 2001, *SciPy: Open Source Scientific Tools for Python*, <http://www.scipy.org/>
- Keenan, R. C., Barger, A. J., Cowie, L. L., & Wang, W.-H. 2010, *ApJ*, **723**, 40
- Kelley, M. S., Fernández, Y. R., Licandro, J., et al. 2013, *Icar*, **225**, 475
- Kipping, D. M., Fossey, S. J., Campanella, G., Schneider, J., & Tinetti, G. 2010, in *ASP Conf. Ser.*, **430**, *Pathways Towards Habitable Planets*, ed. V. Coudé du Foresto, D. M. Gelino, & I. Ribas (San Francisco, CA: ASP), 139
- Leinert, C., Bowyer, S., Haikala, L. K., et al. 1998, *A&AS*, **127**, 1
- Levenson, L. R., Wright, E. L., & Johnson, B. D. 2007, *ApJ*, **666**, 34
- Liou, J.-C., Zook, H. A., & Dermott, S. F. 1996, *Icar*, **124**, 429
- Liou, J.-C., Zook, H. A., & Jackson, A. A. 1995, *Icar*, **116**, 186
- Madau, P., & Pozzetti, L. 2000, *MNRAS*, **312**, L9
- Mather, J. C., & Beichman, C. A. 1996, in *AIP Conf. Ser.*, **348**, ed. E. Dwek, 271
- Matsumoto, T., Matsuura, S., Murakami, H., et al. 2005, *ApJ*, **626**, 31
- Matsuoka, Y., Ienaka, N., Kawara, K., & Oyabu, S. 2011, *ApJ*, **736**, 119
- Matsuura, S., Yano, H., Yonetoku, D., et al. 2014, *Transactions of the Japan Society for Aeronautical and Space Sciences, Aerospace Technology Japan*, **12**, Tr_1
- Matsuura, S., Arai, T., Bock, J. J., et al. 2017, *ApJ*, **839**, 7
- Mattila, K. 2003, *ApJ*, **591**, 119
- Mattila, K. 2006, *MNRAS*, **372**, 1253
- Mattila, K., Lehtinen, K., Väisänen, P., von Appen-Schnur, G., & Leinert, C. 2012, in *IAU Symp.*, **284**, ed. R. J. Tuffs & C. C. Popescu, 429–36 *The Spectral Energy Distribution of Galaxies—SED 2011*
- Mattila, K., Väisänen, P., Lehtinen, K., von Appen-Schnur, G., & Leinert, C. 2017, *MNRAS*, **470**, 2152
- Metzger, B. D. 2017, arXiv:1710.05931
- Morgan, F., Conard, S. J., Weaver, H. A., et al. 2005, *Proc. SPIE*, **5906**, 421
- Moses, J. I. 1992, *Icar*, **99**, 368
- Moses, J. I., Lellouch, E., Bézard, B., et al. 2000, *Icar*, **145**, 166
- Moses, J. I., & Poppe, A. R. 2017, *Icar*, **297**, 33
- Mroz, P., Ryu, Y.-H., Skowron, J., et al. 2017, arXiv:1712.01042
- Muraki, Y., Han, C., Bennett, D. P., et al. 2011, *ApJ*, **741**, 22
- Murthy, J. 2009, *A&SS*, **320**, 21
- Murthy, J. 2016, *MNRAS*, **459**, 1710
- Murthy, J., Hall, D., Earl, M., Henry, R. C., & Holberg, J. B. 1999, *ApJ*, **522**, 904
- Murthy, J., Henry, R. C., & Holberg, J. B. 1991, *ApJ*, **383**, 198
- Murthy, J., Henry, R. C., Shelton, R. L., & Holberg, J. B. 2001, *ApJL*, **557**, L47
- Murthy, J., Im, M., Henry, R. C., & Holberg, J. B. 1993, *ApJ*, **419**, 739
- Nesvorný, D., Vokrouhlický, D., Pokorný, P., & Janches, D. 2011, *ApJ*, **743**, 37
- Nicholl, M., Berger, E., Margutti, R., et al. 2017, *ApJL*, **845**, L8
- Nissanke, S., Kasliwal, M., & Georgieva, A. 2013, *ApJ*, **767**, 124
- Noble, M. W., Conard, S. J., Weaver, H. A., Hayes, J. R., & Cheng, A. F. 2009, *Proc. SPIE*, **7441**, 74410Y
- Oliphant, T. E. 2006, *A Guide to NumPy (USA: Trelgol Publishing)*
- Olkin, C. B., Reuter, D., Lunsford, A., Binzel, R. P., & Stern, S. A. 2006, *BAAS*, **38**, 597, *AAS/Division for Planetary Sciences Meeting Abstracts #38*
- Pan, Y.-C., Kilpatrick, C. D., Simon, J. D., et al. 2017, *ApJL*, **848**, L30
- Perez, F., & Granger, B. E. 2007, *CSE*, **9**, 21
- Pian, E., D'Avanzo, P., Benetti, S., et al. 2017, *Natur*, **551**, 67
- Poleski, R. 2016, *MNRAS*, **455**, 3656
- Poppe, A., & Horányi, M. 2011, *P&SS*, **59**, 1647
- Poppe, A., James, D., Jacobsmeier, B., & Horányi, M. 2010, *GeoRL*, **37**, L11101
- Poppe, A. R. 2016, *Icar*, **264**, 369
- Quinten, M., Kreibig, U., Henning, T., & Mutschke, H. 2002, *ApOpt*, **41**, 7102

- Reuter, D. C., Stern, S. A., Scherrer, J., et al. 2008, *SSRv*, **140**, 129
- Rice, K. 2014, *Chall*, **5**, 296
- Rogers, G., Schwinger, M., Kaidy, J., et al. 2006, Autonomous Star Tracker Performance for the New Horizons Mission (American Institute of Aeronautics and Astronautics), <https://doi.org/10.2514/6.2006-6383>
- Rybicki, G. B., & Lightman, A. P. 1986, *Radiative Processes in Astrophysics* (Weinheim: Wiley-VCH)
- Sano, K., Kawara, K., Matsuura, S., et al. 2015, *ApJ*, **811**, 77
- Singer, L. P., Chen, H.-Y., Holz, D. E., et al. 2016, *ApJL*, **829**, L15
- Stern, S. A. 1996, *A&A*, **310**, 999
- Stern, S. A., Weaver, H. A., Spencer, J. R., & Elliott, H. A. 2018, *SSRv*, **214**, 77
- Stern, S. A., Slater, D. C., Scherrer, J., et al. 2008, *SSRv*, **140**, 155
- Stone, E., Alkalai, L., Friedman, L., et al. 2015, Science and Enabling Technologies for the Exploration of the Interstellar Medium, Tech. rep. (Pasadena, CA: Keck Inst. for Space Studies)
- Street, R. A., Udalski, A., Calchi Novati, S., et al. 2016, *ApJ*, **819**, 93
- Sullivan, P. W., Winn, J. N., Berta-Thompson, Z. K., et al. 2015, *ApJ*, **809**, 77
- Sumi, T., & Penny, M. T. 2016, *ApJ*, **827**, 139
- Szalay, J. R., Piquette, M., & Horányi, M. 2013, *EP&S*, **65**, 1145
- Toller, G., Tanabe, H., & Weinberg, J. L. 1987, *A&A*, **188**, 24
- Toller, G. N. 1983, *ApJL*, **266**, L79
- Totani, T., Yoshii, Y., Iwamuro, F., Maihara, T., & Motohara, K. 2001, *ApJL*, **550**, L137
- Tsapras, Y., Hundertmark, M., Wyrzykowski, L., et al. 2016, *MNRAS*, **457**, 1320
- Tsumura, K., Matsumoto, T., Matsuura, S., Sakon, I., & Wada, T. 2013, *PASJ*, **65**, 121
- Tyson, J. A. 1995, in *Extragalactic Background Radiation Meeting*, ed. D. Calzetti, M. Livio, & P. Madau, 103–33
- Valenti, S., Sand, D. J., Yang, S., et al. 2017, *ApJL*, **848**, L24
- Vanderburg, A., & Johnson, J. A. 2014, *PASP*, **126**, 948
- Verbiscer, A. J., Skrutskie, M. F., & Hamilton, D. P. 2009, *Natur*, **461**, 1098
- Villanueva, S., Jr., Dragomir, D., & Gaudi, B. S. 2018, [arXiv:1805.00956](https://arxiv.org/abs/1805.00956)
- Vitense, C., Krivov, A. V., Kobayashi, H., & Löhne, T. 2012, *A&A*, **540**, A30
- Vitense, C., Krivov, A. V., & Löhne, T. 2010, *A&A*, **520**, A32
- Warren, S. G. 1984, *ApOpt*, **23**, 1206
- Weaver, H. A., Gibson, W. C., Tapley, M. B., Young, L. A., & Stern, S. A. 2008, *SSRv*, **140**, 75
- Weinberg, J. L., Hanner, M. S., Beeson, D. E., DeShields, L. M., II, & Green, B. A. 1974, *JGR*, **79**, 3665
- Wright, E. L. 2001, *ApJ*, **553**, 538
- Wright, E. L. 2004, *NewAR*, **48**, 465
- Wyrzykowski, L., Skowron, J., Kozłowski, S., et al. 2011, *MNRAS*, **416**, 2949
- Yee, J. C., Gould, A., Beichman, C., et al. 2015, *ApJ*, **810**, 155
- Zemcov, M., Immel, P., Nguyen, C., et al. 2017, *NatCo*, **8**, 15003
- Zemcov, M., Smidt, J., Arai, T., et al. 2014, *Sci*, **346**, 732
- Zhu, W., Udalski, A., Huang, C. X., et al. 2017a, *ApJL*, **849**, L31
- Zhu, W., Huang, C. X., Udalski, A., et al. 2017b, *PASP*, **129**, 104501